DOT/FAA/TC-19/51

Federal Aviation Administration
William J. Hughes Technical Center
Aviation Research Division
Atlantic City International Airport
New Jersey 08405

A Survey of Wire Strike Prevention and Protection Technologies for Helicopters

January 2019

U.S. Department of Transportation
Federal Aviation Administration

NOTICE

Technical Report Documentation Page

1. Report No.	2. Government Accession No.	3. Recipient's Catalog No.
DOT/FAA/AR-19/51		

4. Title and Subtitle	5. Report Date
A SURVEY OF WIRE STRIKE PREVENTION AND PROTECTION TECHNOLOGIES FOR HELICOPTERS	January 2019
	6. Performing Organization Code
7. Author(s)	8. Performing Organization Report No.
Ruthvik Chandrasekaran, Alexia Payan, Kyle Collins, and Dimitri Mavris	
9. Performing Organization Name and Address	10. Work Unit No. (TRAIS)
Aerospace Systems Design Laboratory The Daniel Guggenheim School of Aerospace Engineering Georgia Institute of Technology 281 Ferst Drive NW, Atlanta, GA 30332	
	11. Contract or Grant No.
12. Sponsoring Agency Name and Address	13. Type of Report and Period Covered
Federal Aviation Administration William J. Hughes Technical Center Atlantic City International Airport Atlantic City, NJ 08405	Final Report 08/30/2018-01/31/2019
	14. Sponsoring Agency Code

15. Supplementary Notes

The Federal Aviation Administration Aviation William J. Hughes Technical Center Research Division COR was Traci Stadtmueller and Paul Swindell.

16. Abstract

Rotorcraft typically operate at low altitudes and this puts them at risk of striking various types of obstacles. Studies reveal that wire strikes are a major source of helicopter accidents often leading to fatalities. Data on civil helicopter wire strike accidents further show that a majority of helicopter models involved fall in the light and intermediate weight categories. In this report, existing wire strike prevention and protection technologies for rotorcraft are reviewed. In particular, commercially available wire detection systems such as laser- and radar-based scanning systems, database-dependent prevention systems, wire cutters, and wire/aerial markers are surveyed and evaluated against each other. Publicly available databases of transmission lines and cable construction materials in the U.S. are identified and documented for the development of wire strike prevention technologies for lightweight helicopters. The feasibility of creating useful maps of wires from tabulated data or image data is discussed and various Electronic Flight Bag (EFB) manufacturers are surveyed to determine the feasibility of integrating and displaying such information. Finally, existing wire cutter systems, patents, and experimental studies are examined to understand the working concepts of different wire cutter protection systems, and the challenges and obstacles related to the implementation of a wire cutter system on lightweight rotorcraft are identified.

17. Key Words	18. Distribution Statement
	This document is available to the U.S. public through the National Technical Information Service (NTIS), Springfield, Virginia 22161. This document is also available from the Federal Aviation Administration William J. Hughes Technical Center at actlibrary.tc.faa.gov.

19. Security Classif. (of this report)	20. Security Classif. (of this page)	21. No. of Pages	22. Price
Unclassified	Unclassified		

Form DOT F 1700.7 (8-72) Reproduction of completed page authorized

TABLE OF CONTENTS

LIST OF FIGURES

Page

LIST OF TABLES

Page

LIST OF ACRONYMS

AAAC	All Aluminum Alloy Conductor
ACAR	Aluminum Conductor Alloy Reinforced
ACSR	Aluminum Conductor Steel Reinforced
ACSR/TW	Trapezoidal Aluminum Alloy Conductor Steel Reinforced
ASTM	American Society for Testing and Materials
AWG	American Wire Gauge
CASA	Civil Aviation Safety Authority
EASA	European Aviation Safety Agency
EFB	Electronic Flight Bag
EHV	Extra High Voltage
EIA	Energy Information Administration
FAA	Federal Aviation Administration
FEM	Finite Element Method
FOV	Field of View
FRAT	Flight Risk Assessment Module
HELLAS	Helicopter Laser Radar
HMW	High Molecular Weight
HV	High Voltage
LIDAR	Light Imaging Detection and Ranging
LOAM	Laser Obstacle Avoidance System
ML	Machine Learning
NOE	Nap Of the Earth
OAWS	Obstacle Avoidance and Warning System
OCAS	Obstacle Collison Avoidance System
OCC	OCAS Control Center
PDS	Power line Detection System
TAWS	Terrain Awareness and Warning System
ToF	Time of Flight
UAV	Unmanned Aerial Vehicle
VFR	Visual Flight Rules
WSPS	Wire Strike Protection System
WSPT	Wire Strike Prevention Technology
XFEM	Extended FEM

EXECUTIVE SUMMARY

Helicopters typically operate at low altitudes, putting them at risk of striking various obstacles. Studies reveal that wire strikes are a major source of helicopter accidents, often leading to fatalities. Data on civil-helicopter wire-strike accidents show that a majority of the helicopters involved in accidents are in the light and intermediate weight categories. In this report, existing wire-strike prevention and protection technologies for helicopters are reviewed. Commercially available wire-detection systems such as laser- and radar-based scanning systems, database-dependent prevention systems, wire cutters, and wire/aerial markers are surveyed and evaluated against each other. Publicly available databases of transmission lines and cable-construction materials used in the U.S. are identified and documented for the development of wire-strike prevention technologies for lightweight helicopters. The feasibility of creating useful maps of wires from tabulated data or image data is discussed, and various Electronic Flight Bag (EFB) manufacturers are surveyed to determine the feasibility of integrating and displaying such information. Finally, existing wire-cutter systems, patents, and experimental studies are examined to understand the working concepts of different wire-cutter protection systems, and the challenges and obstacles of implementing a wire-cutter system on lightweight helicopters are identified.

1. INTRODUCTION

Wire strikes are a major source of helicopter accidents. A study from the Federal Aviation Administration (FAA) showed that wire-strike accidents accounted for five percent of all the accidents that occurred from 1963 to 2008 (Nagaraj & Chopra, 2008). Among these five percent, a third of the wire-strike accidents involving civil helicopters between 1994 and 2004 were fatal and mostly occurred in clear, daytime, Visual Flight Rules (VFR) conditions.

Wire-strike accidents typically occur during low-altitude operations below a thousand feet. Since helicopters operate within this region for prolonged periods of time, they are highly susceptible to wire-strike accidents. They are also highly prone to wire strikes during take-off and landing. In particular, military helicopters are at higher risks of striking a wire due to sabotage wires and more frequent Nap of the Earth (NOE) flights performed in order to avoid enemy detection, as shown in Figure 1.1.

Figure 1.1: Nap of the Earth Operation[1]

According to accident reports from the National Transportation Safety Board (NTSB) (Nagaraj & Chopra, 2008), the following reasons are stated as the most probable causes of wire strikes:

- Inadequate visual lookout
- Inconspicuousness of power lines
- Failure to maintain sufficient clearance from transmission wires
- Sun glare
- Failure to maintain proper altitude
- Improper Judgement
- Lack of preflight planning
- Darkness and lack of visual cues
- Failure to see and avoid wires
- Selection of unsuitable landing sites

[1] *http://geography.name/nap-of-the-earth/* [Last accessed on 01/31/2019]

Wires can be very difficult to see because of their small size and because they easily blend in with the background. A study of the NTSB wire-strike accident reports between 1994 and 2004 revealed that the 124 wire-strike accidents identified were responsible for 65 fatalities and 87 serious and minor injuries. The number of fatalities per wire strike was thus 0.524. Thirty-seven of the fatal strikes took place in day-visual meteorological conditions, two occurred in day-instrument flying conditions, and two occurred in night instrument flying. Hence, most of the fatal accidents occurred in good visibility, clear weather conditions. Figure 1.2 (a) and (b) show wreckages of helicopters involved in wire-strike accidents.

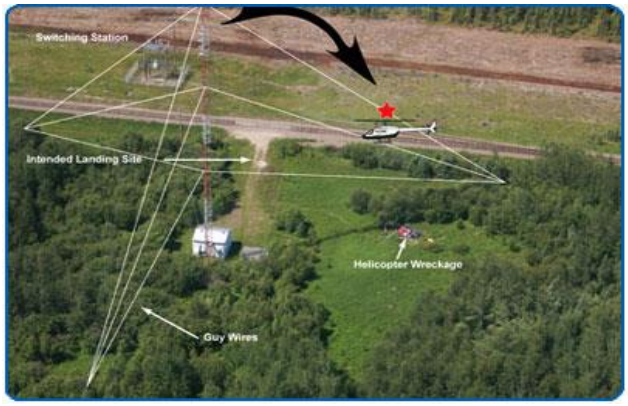

(a): Wreckage of a CHL AS350BA[2] **(b): Wreckage of an Aerospatiale AS 350 B2[3]**

Figure 1.2: Helicopter Wire-Strike Accidents

Data on civil helicopter wire-strike accidents show that a majority of the helicopters involved in accidents are in the lightweight and intermediate-weight categories (Nagaraj & Chopra, 2008). For example, the Robinson R22 accounted for 15.3% of all the accidents, while the Bell 47 and the Bell 206 accounted for 20.2% and 18.6% respectively. The great majority of pilots involved in these accidents were between the ages of 40 and 59, and had more than 2,000 hours of flying experience in helicopters. Most of these accidents may have been prevented if one or more safety devices had been installed onboard the vehicle, to warn the pilot of wires. In addition, helicopters could be equipped with wire cutters to protect the blades from an impending strike if collision with wires becomes unavoidable. Although some helicopters are equipped with wire cutters, not all of them are. In particular, there are currently no-wire cutter solutions for lightweight helicopters. Since many helicopters that are involved in fatal wire-strike accidents are in the lightweight and intermediate-weight categories, it is important to either adapt current devices or develop new wire-cutter systems suitable for these helicopter categories.

This report provides a review of existing databases of wires in the United States, Electronic Flight Bags (EFBs) in which such databases might be implemented, common conductor and guy cables used in the U.S., and various wire-strike prevention and protection technologies based on publicly available literature. Challenges to the implementation of wire cutters on lightweight rotorcraft is studied in detail, along with the fracture mechanics of stranded wires under tension.

[2] http://aerossurance.com/helicopters/fatal-to-wire-strike/ [Last accessed on 01/31/2019]
[3] *https://www.tc.gc.ca/eng/civilaviation/publications/tp185-4-2010-tsb-5891.htm* [Last accessed on 01/31/2019]

2. EXISTING WIRE DATABASES

Most helicopter wire strikes are caused by transmission power lines and communication lines during take-off and landing. Hence, it is important to know the locations and properties of these lines. Such information may then be incorporated into avionics and electronic flight bags to warn pilots of potential collisions.

The bulk of the North American power grid is divided into four distinct parts or interconnections: Eastern Interconnection, Western Interconnection, Electricity Reliability Council of Texas Interconnection, and Quebec Interconnection. Although these interconnections can operate independently, they are connected to each other at certain locations to allow transfer of power when required. The regions that come under each interconnection are shown in Figure 2.1.

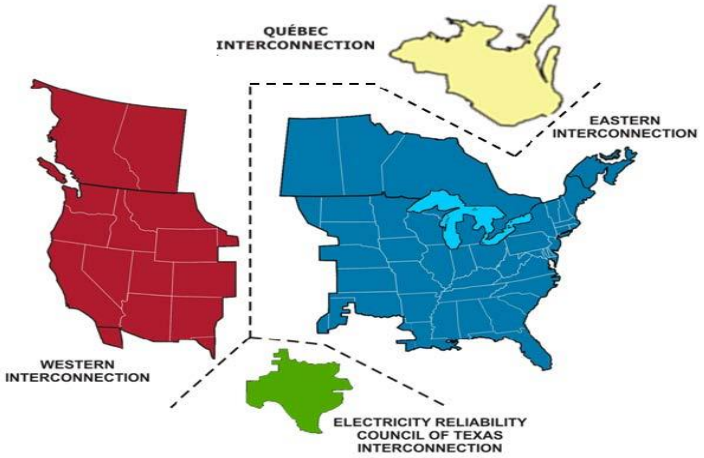

Figure 2.1: North American Interconnections (OEDER, 2015)

Two thirds of the United States and Canada are covered by the Eastern Interconnection. The Western interconnection includes the provinces of Alberta and British Columbia in Canada, the region from the Great Plains to the West Coast of the U.S., and a portion of Baja California Norte in Mexico. The state of Texas in the U.S. and the province of Quebec in Canada have their own independent interconnection due to historical reasons.

Power-generation plants based on fossil fuels, nuclear power, and wind energy and other renewable sources are located at various locations within the interconnection and transmit power through transmission lines. According to the Office of Electricity Delivery and Energy Reliability (OEDER, 2015), power plants generate electricity between 5 and 34.5 kilovolts, which is then transmitted at 69 to 765 kilovolts. Power plants are located at significant distances from the region of demand, hence large voltage differences are required to transfer electricity without significant losses. The entire power grid consists of about 580,000 km of transmission lines operated by approximately 500 companies (OEDER, 2015).

Transmission lines come in different sizes and constructions depending on the voltage requirements of the power grid. Figure 2.2 provides a summary of the power grid voltage distribution.

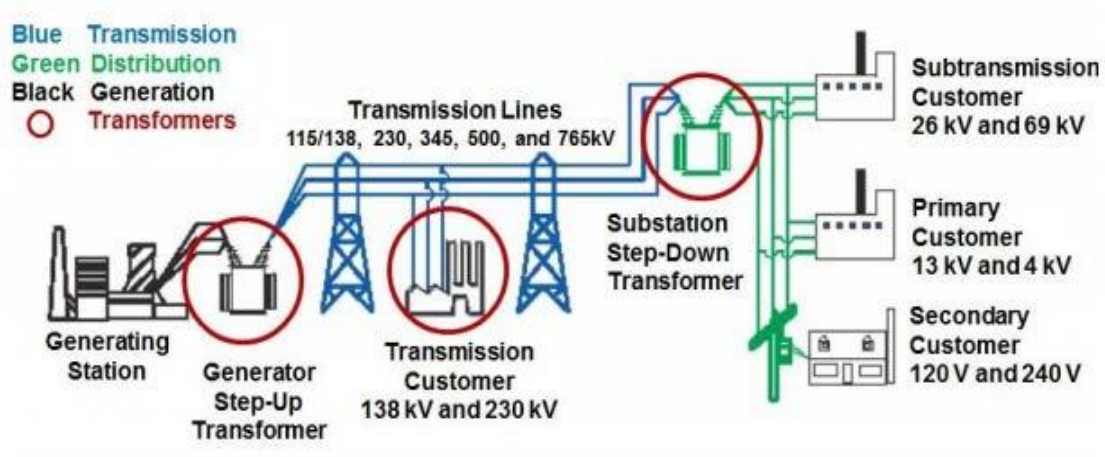

Figure 2.2: Voltage Distribution in the Power-Grid (OEDER, 2015)

Several databases describing the locations and voltage readings of these transmission lines are available. The Federal Emergency Management Agency (FEMA) provides a map, shown in Figure 2.3, of the network of High Voltage – HV (100 kV – 200 kV), and Extra High Voltage – EHV (200kV – 800 kV), power lines across the U.S.

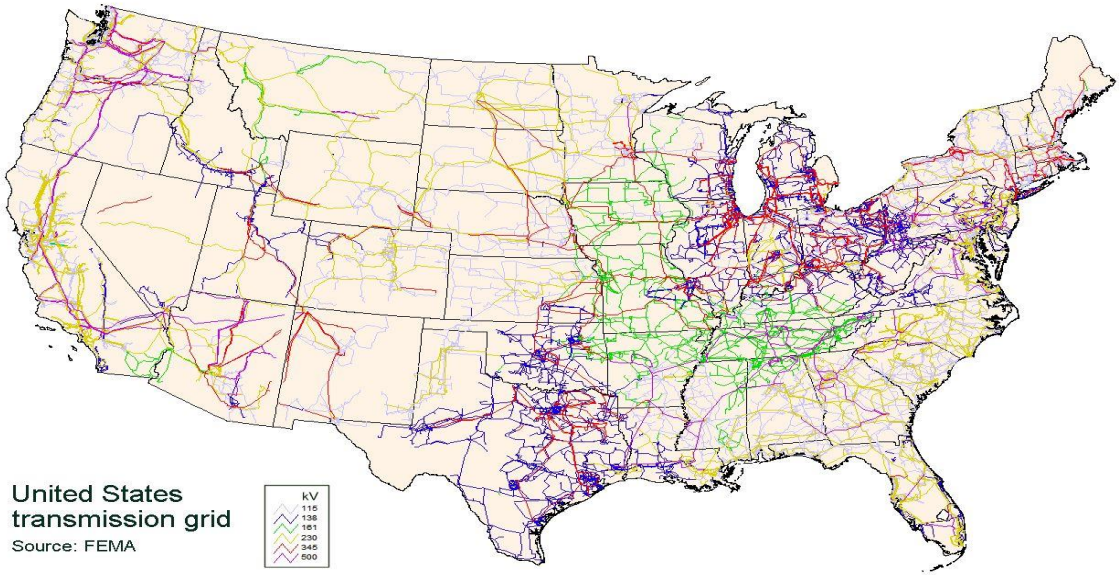

Figure 2.3: Map of the U.S. Power-Grid[4]

A more detailed and interactive database is available from the U.S. Energy Information Administration (EIA). This database is shown in Figure 2.4 and Figure 2.5. This database provides the locations and voltage readings of power lines across the U.S., and for each transmission line, the service status, operating company, and substation to which it is connected.

[4] *https://en.wikipedia.org/wiki/Continental_U.S._power_transmission_grid* [Last accessed on 01/31/2019]

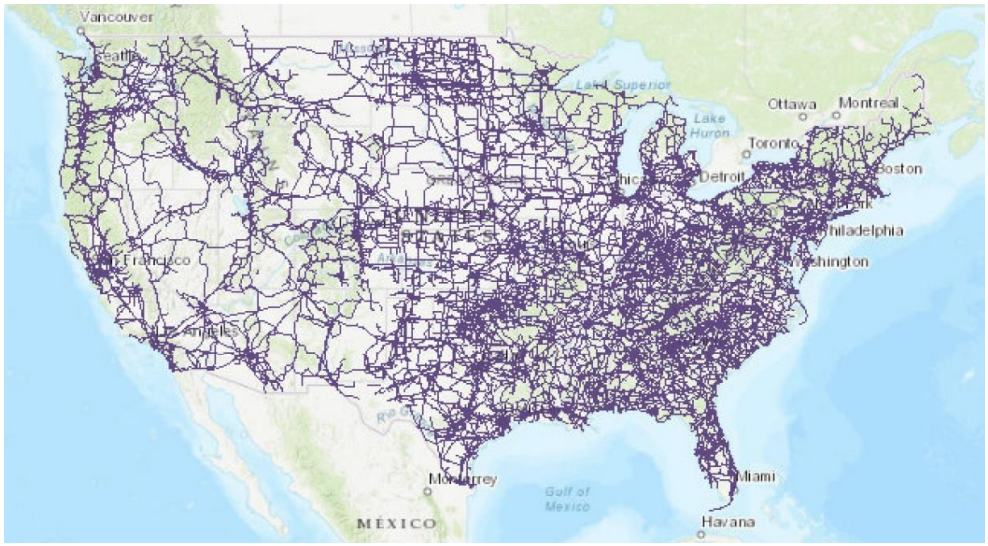

Figure 2.4: Interactive Map of the U.S. Power-Grid[5]

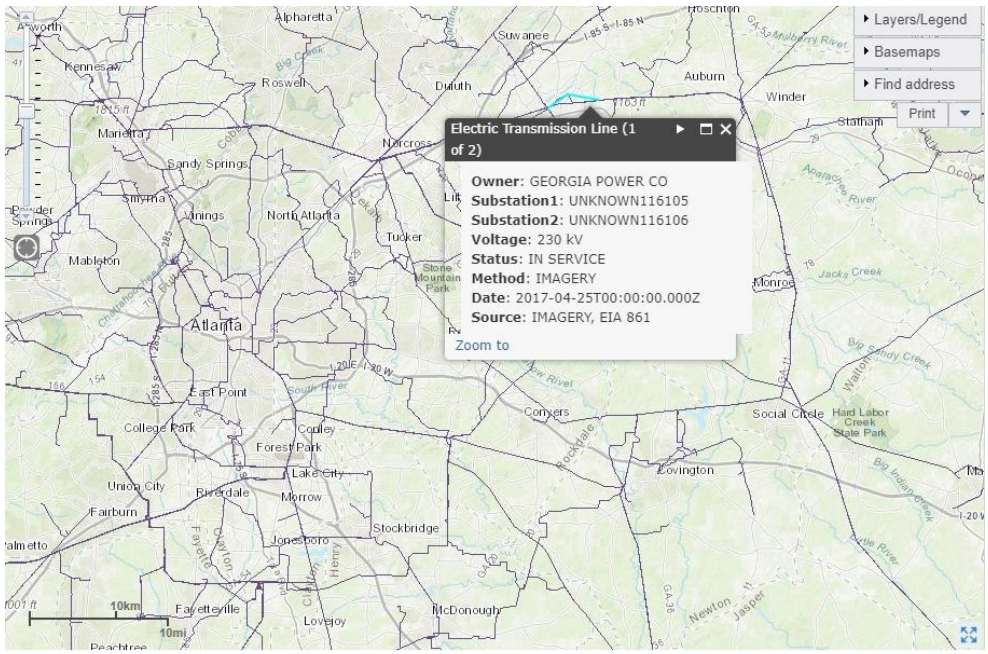

Figure 2.5: Interactive Map of the U.S. Power-Grid Showing Power line Information[6]

Less detailed maps covering power lines of high voltage (HV) and extra high voltage (EHV) are shown in Figure 2.6 and Figure 2.7.

[5] *https://www.eia.gov/state/maps.php* [Last accessed on 01/31/2019]
[6] *https://www.eia.gov/state/maps.php* [Last accessed on 01/31/2019]

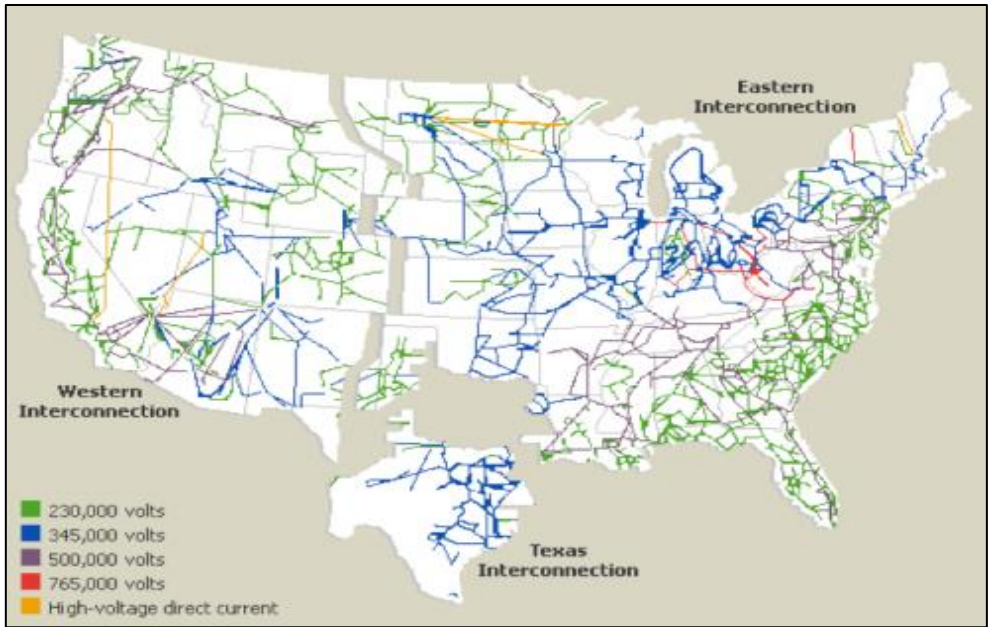

Figure 2.6: Transmission Lines Above and Below 500 kV[7]

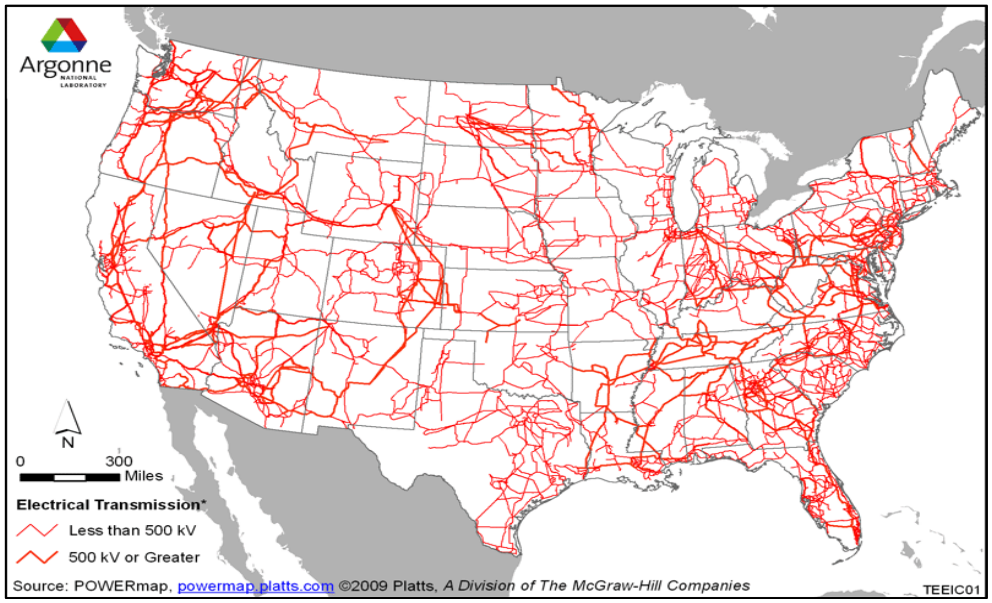

Figure 2.7: Transmission Lines in the EHV Range[8]

The Digital Obstacle File (DOF) on the FAA website provides metadata on obstacles that could be a threat to aircraft and rotorcraft operators. The metadata are in several DAT files, one for each U.S. state, and one for some obstacles in Canada, the Bahamas, the Caribbean, Mexico, the Pacific, and Puerto Rico (Federal Aviation Administration, 2018). This metadata includes

[7] *https://judithcurry.com/2015/05/07/transmission-planning-wind-and-solar/* [Last accessed on 01/31/2019]
[8] *http://www.mojavedesertblog.com/2013/07/how-much-more-transmission-do-we-need.html* [Last accessed on 01/31/2019]

coordinates, location name, height (above ground level), type, and several other properties of the obstacles; however, most of the available data is concentrated near big cities and airports. Figure 2.8 shows, for the state of Alabama, the catenary (power lines) data as red dots.

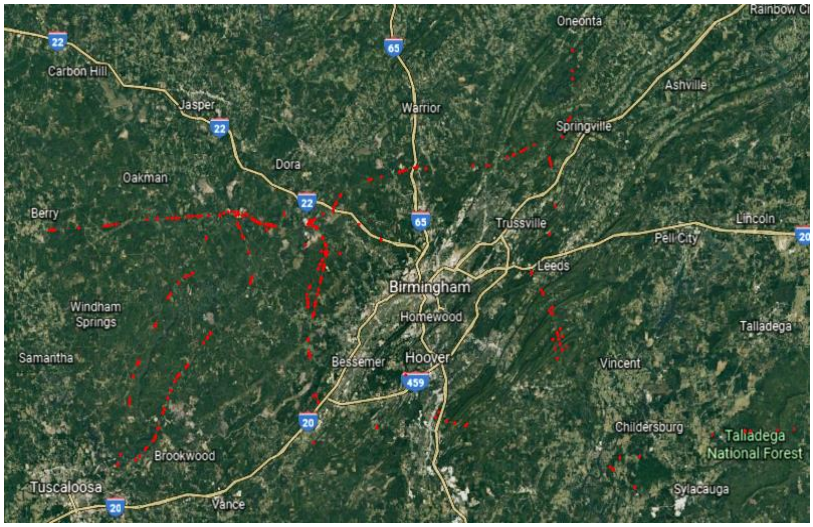

Figure 2.8: Power line (Catenary) Data Plotted in Google Earth

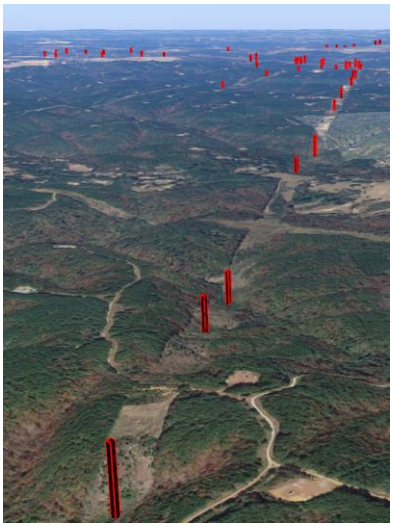

Figure 2.9: Cylinders Representing Catenary Height in Google Earth

Figure 2.9 shows the heights of the catenaries as red cylinders. These figures show that such catenary data may be used to create a map of transmission lines in the U.S.; however, only discrete locations along transmission lines are provided in the database. Connections should be made appropriately to track the path of these lines. This can be done manually or with image-processing techniques.

Even if all the necessary data is available in the database, creating maps manually over large areas is a time-consuming and monotonous process. If all the necessary data is not available, creating such maps manually is even more difficult if one must use satellite imagery to identify power lines. In such a scenario, machine learning (ML) algorithms have been used to accelerate the process. For example, power-grid maps of Pakistan, Nigeria, and Zambia have been created using satellite images and machine-learning techniques (Development Seed, 2018). This project used the fact that high voltage (HV) towers are the most striking and easily identifiable feature of the power-grid system. Xception, a convolutional neural network, was trained to identify HV towers in different terrains. The neural network predicts the existence of a HV tower inside a region and draws a box enclosing the area as show in Figure 2.10. The corresponding power-grid map can be obtained by connecting the towers inside these locations manually and may be overlaid on satellite images.

Figure 2.10: ML Algorithm Prediction of HV Tower Locations[9]

Although the ML algorithm is not 100% accurate in identifying towers, the number of correct predictions significantly outweigh the set of false predictions. Furthermore, knowing the location of towers saves a tremendous amount of time for mappers. Using an ML algorithm to predict tower locations increased mapping speed by almost seventeen times. A group of eight professional mappers were able to process 120 km^2 per hour without ML, but the speed increased to 2035 km^2 per hour when ML was used. The mapping rates for the manual method and for the automated method are compared in Figure 2.11.

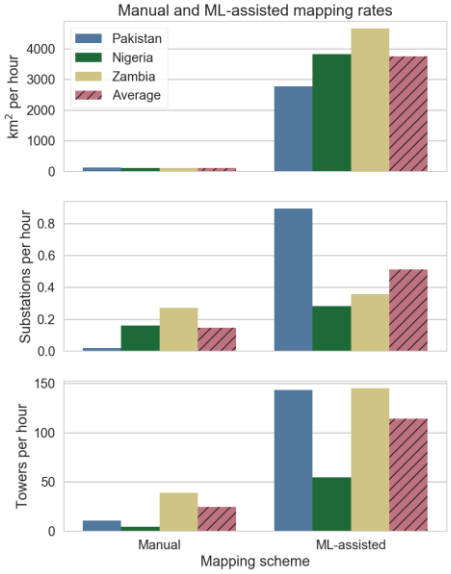

Figure 2.11: Comparison of Mapping Methods (Development Seed, 2018)

[9] *https://developmentseed.org/blog/2018/02/15/hv-grid/* [Last accessed on 01/31/2019]

3. CABLES IN THE UNITED STATES

There are several databases providing information about cables used in the U.S. One of the most comprehensive databases is provided by the American Wire Group (American Wire Group, 2018), a Florida-based wire and cable company. This database includes information about guy wires, telephone wires, and electrical-transmission cables. The Aluminum Association (The Aluminum Association, 1999) also provides a report explaining the British, Canadian, and U.S. codes used to describe overhead aluminum electrical conductors. The French company Nexans (Nexans, 2003) provides information about the most common bare overhead conductors and their associated codes.

Due to the plethora of cables and sources of information about them, only certain cables and their mechanical properties will be discussed in the following sections.

3.1 STATIC WIRES

A static wire is a wire connected to the top of a utility pole that serves as a safety mechanism during lightning strikes. It is connected to a ground rod through a grounding connector wire that runs along the utility pole from top to bottom, as shown in Figure 3.1.

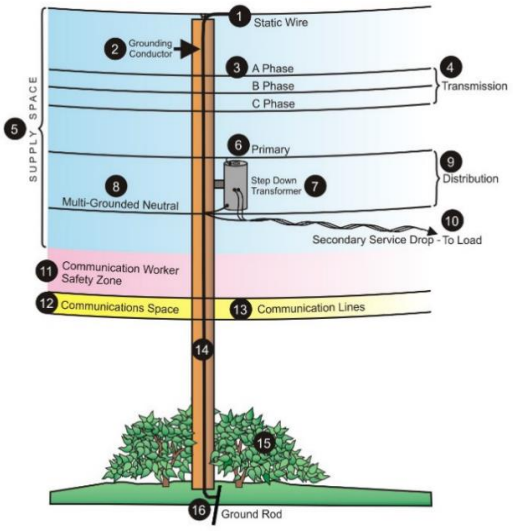

Figure 3.1: Static Wire at the Top of a Pole[10]

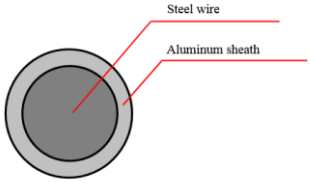

Figure 3.2: Alumoclad Steel Strand[11]

Figure 3.3: Static Wire Construction (American Wire Group, 2018)

A static wire is made up of a material with low electrical resistance, which provides a path for lightning surges to reach ground. Each strand in a static wire has a steel core with a thin protective layer of aluminum on its surface, as depicted in Figure 3.2. The metals are bonded together by a process called "cladding". Hence, the wire is called Alumoclad steel wire. Alumoclad steel wires have very good corrosion resistance and great strength. This leads to long fatigue life. Depending on the number and the size of steel/aluminum strands used in a wire, as depicted in Figure 3.3, the wire is assigned a different name. Various types of static wires and their properties are summarized in Table 3.1.

[10] *http://www.psc.state.fl.us/ConsumerAssistance/UtilityPole* [Last accessed on 01/31/2019]
[11] *http://en.sarko.ru/aluminium-clad-steel-wire.html* [Last accessed on 01/31/2019]

Table 3.1: Alumoclad Steel Static Wire Types and Properties (American Wire Group, 2018)

Name	No. and Size of wire (AWG Standard)	Nominal Diameter (in)	Cross Sectional Area (in^2)	Weight (lb/MFT) 1 MFT = 10^3 ft	Tensile Breaking Load (lb)
ALUM-01	37#5	1.270	0.96152	2802	142800
ALUM-02	37#6	1.130	0.76264	2222	120200
ALUM-03	37#7	1.010	0.60509	1762	100700
ALUM-04	37#8	0.899	0.47984	1398	84200
ALUM-05	37#9	0.801	0.38032	1108	66770
ALUM-06	37#10	0.713	0.30174	879	52950
ALUM-07	19#5	0.910	0.49438	1430	73350
ALUM-08	19#6	0.810	0.39163	1134	61700
ALUM-09	19#7	0.721	0.31073	899.5	51730
ALUM-10	19#8	0.642	0.24641	713.5	43240
ALUM-11	19#9	0.572	0.1953	565.8	34290
ALUM-12	19#10	0.509	0.15495	448.7	27190
ALUM-13	7#5	0.546	0.18193	524.9	27030
ALUM-14	7#6	0.486	0.14435	416.3	22730
ALUM-15	7#7	0.433	0.11448	330	19060
ALUM-16	7#8	0.385	0.09077	261.8	15930
ALUM-17	7#9	0.343	0.07198	207.6	12630
ALUM-18	7#10	0.306	0.05708	164.7	10020
ALUM-19	7#11	0.272	0.04527	130.6	7945
ALUM-20	7#12	0.242	0.0359	103.6	6301
ALUM-21	3#5	0.392	0.07796	224.5	12230
ALUM-22	3#6	0.349	0.06185	178.1	10280
ALUM-23	3#7	0.311	0.04905	141.2	8621
ALUM-24	3#8	0.277	0.0389	112	72060
ALUM-25	3#9	0.247	0.03085	888.1	5715
ALUM-26	3#10	0.220	0.02446	704.3	4532
ALUM-27	#4	0.2043	0.03278	936.3	5081
ALUM-28	#5	0.1819	0.02599	742.5	4290
ALUM-29	#6	0.1620	0.02062	588.8	3608
ALUM-30	#7	0.1443	0.01635	466.9	3025
ALUM-31	#8	0.1285	0.01297	370.3	2529
ALUM-32	#9	0.1144	0.01028	293.7	2005
ALUM-33	#10	0.1019	0.00816	232.9	1590
ALUM-34	#11	0.0907	0.00647	184.7	1261
ALUM-35	#12	0.0808	0.00513	146.5	1000

*****Refer to (American Wire Group, 2018) for additional wire types and properties.

Nomenclature:

No.: Number of strands used in a wire

Size of wire: #X (X is the size of a strand according to AWG standard, see Appendix a – AWG Standards)

3.2 GUY WIRES

A guy wire is a cable that adds stability to a free-standing structure. It is a tension cable attached from the structure to the ground, as depicted in
Figure 3.4. Guy wires are used in radio masts, utility poles, ship masts, wind turbines, and tents.

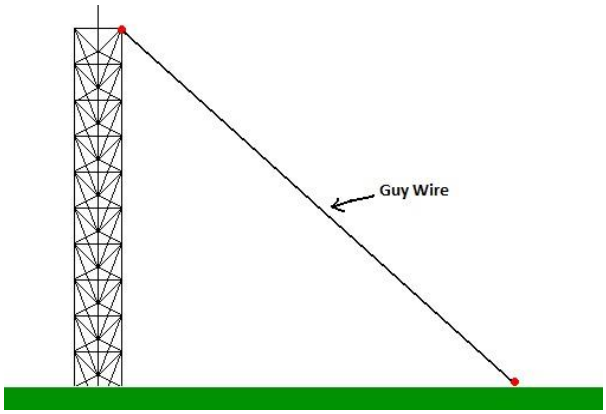

Figure 3.4: Guy Wire[12]

Guy wires are made of alumoclad steel strands of Type M, which have a guaranteed aluminum cladding thickness of more than 10% of the wire radius. This thick aluminum layer protects the steel core from corrosion. The aluminum layer and the steel core are joined by a continuous ductile weld that prevents cracking and separation. Type M alumoclad has high strength and low weight. Table 3.2 provides properties for Type M guy wires.

Table 3.2: Type M Alumoclad Steel Guy Wire Types and Properties (American Wire Group, 2018)

Name	No. of Strands/ Diameter of a Strand (in)	Nominal Diameter (in)	Cross Sectional Area (in^2)	Weight (lb/MFT) 1 MFT = 10^3 ft	Tensile Breaking Load (lb)
AGM-19	7/0.173	0.519	0.1645	474.8	25,000
AGM-18	7/0.165	0.5	0.1497	432	22,900
AGM-17	7/0.148	0.444	0.1204	347.5	20,000
AGM-16	7/0.145	0.4375	0.1156	333.6	18,700
AGM-15	7/0.139	0.417	0.1062	306.6	18,000
AGM-14	7/0.128	0.386	0.0901	260	16,000
AGM-13	7/0.121	0.363	0.0805	232.2	14,100
AGM-12	7/0.121	0.375	0.0792	228	13,800
AGM-11	7/0.114	0.343	0.0714	206.2	12,500
AGM-10	7/0.110	0.330	0.0665	192	11,600
AGM-9	7/0.104	0.3125	0.0595	171.6	10,400
AGM-8	7/0.102	0.306	0.0572	165.1	10,000
AGM-7	3/0.141	0.3125	0.0495	142.7	8,400
AGM-6	7/0.191	0.272	0.0455	131.4	8,000
AGM-5	3/0.128	0.277	0.0386	111.2	7,100
AGM-4	7/0.083	0.249	0.0379	109.3	6,600
AGM-3	7/0.081	0.242	0.0361	104.1	6,300
AGM-2	3/0.114	0.247	0.0306	88.18	5,600
AGM-1	3/0.102	0.22	0.0245	70.61	4,500

*****Refer to (American Wire Group, 2018) for additional wire types and properties

[12] *http://www.hamuniverse.com/guywirelengthformula.html*

Static and guy wires, in certain cases, also could be made of galvanized steel, which has superior corrosive coating and high strength. Some details are provided in Table 3.3. Galvanized steel wires can also be used as messenger wires, which are secondary wires attached to the wires that carry signals. The job of a messenger wire is to provide additional strength and reduce sagging of overhead wires.

Table 3.3: Galvanized Steel Guy/Static/Messenger Wire Types and Properties (American Wire Group, 2018)

Name	Nominal Diameter (in)	No. of Strands	Common Grade Tensile Breaking Strength (lb)	High Strength Grade Tensile Breaking Strength (lb)
GW5-3/16-062	3/16	7	1150	2850
GW7-7/32-072	7/32	7	1540	3850
GW8-1/4-080	1/4	7	1900	4750
GW9-9/32-093	9/32	7	2570	6400
GW10-5/16-104	5/16	7	3200	8000
GW12-3/8-120	3/8	7	4250	10800
GW13-7/16-145	7/16	7	5700	14500
GW14-1/2-165	1/2	7	7400	18800
GW15-9/16-188	9/16	7	9600	24500
GW16-5/8-207	5/8	7	11600	29600
GW17-1/2-100	1/2	19	7620	19100
GW18-9/16-113	9/16	19	9640	24100
GW19-5/8-125	5/8	19	11000	28100
GW20-3/4-150	3/4	19	16000	40800
GW21-7/8-177	7/8	19	21900	55800
GW22-1-200	1	19	28700	73200

3.3 TELEPHONE WIRES

Telephone wires are made of copperclad steel wires covered with high olecular weight (HMW) polyethylene, as shown in Figure 3.5. Copperclad steel is a steel wire cladded with copper as shown in Figure 3.6. The steel core provides mechanical strength and the copper provides electrical conductivity. Details on telephone wires can be found in Table 3.4.

Figure 3.5: Telephone Line Wire Construction[13]

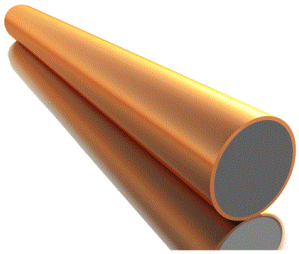

Figure 3.6: Copperclad Steel[14]

Table 3.4: Copperclad Telephone Wire Types and Properties (American Wire Group, 2018)

Name	Conductivity (Depends on Anneal Process)	Diameter of Wire (in)	Covering Thickness (in)	Weight (lb/MFT) 1 MFT = 10^3 ft	Tensile Breaking Load (lb)
PCSC-6-30	30%	0.1620	0.03125	80.3	2680
PCSC-8-30	30%	0.1285	0.03125	51.8	1815
PCSC-9-30	30%	0.1144	0.03125	41.7	1491
PCSC-10-30	30%	0.1019	0.03125	33.9	1231
PCSC-6-40	40%	0.1620	0.03125	80.3	2433
PCSC-8-40	40%	0.1285	0.03125	51.8	1660
PCSC-9-40	40%	0.1144	0.03125	41.7	1368
PCSC-10-40	40%	0.1019	0.03125	33.9	1130
PCSC-12-40	40%	0.08081	0.03125	22.3	785

[13] http://wire.buyawg.com/item/polyethylene-solid-copper-clad-steel-wire/polyethylene-covered-solid-copper-clad-steel-wire/pcsc-9-30 [Last accessed on 01/31/2019]

[14] *http:/www.generalclad.com/product-category/sample-product/ccs-32/* [Last accessed on 01/31/2019]

3.4 ELECTRICAL TRANSMISSION AND DISTRIBUTION CABLES

Electrical-transmission cables, also known as conductors, are made of aluminum and steel, due to their mechanical properties and low costs. Although copper is a better conductor than aluminum and has a very high corrosion resistance, it is not widely used due to high material costs. Depending on their construction, conductor wires are classified as follows:

- Aluminum Conductor Steel Reinforced (ACSR)
- All Aluminum Alloy Conductor (AAAC)
- Aluminum Conductor Alloy Reinforced (ACAR)
- Trapezoidal Aluminum Alloy Conductor Steel Reinforced (ACSR/TW)

Overhead conductors are not insulated to reduce their costs and weights. Less weight leads to less sagging when the conductors are connected to the transmission tower. This leads to shorter towers, thus reducing costs further. (A slight amount of sag is preferred to reduce vibratory loads during windy conditions.)

An international standard nomenclature does not exist for overhead conductors but different code names are assigned to them in different regions of the world as follows:

- ACSR – Based on animals – UK
- ACSR – Based on birds – North America
- AAAC – Based on insects – UK
- AAAC – Based on flowers – North America

3.4.1 Aluminum Conductor Steel Reinforced (ACSR)

Most of the ACSR cables have a steel core made up of one or more steel strands, wrapped by aluminum strands in a helical motion. They are mainly used as primary and secondary transmission cables. Desired strengths can be achieved by varying the steel-core stranding. Typical ACSR cable cross-sections are shown in Figure 3.7.

Outer strands are composed of aluminum alloy 1350-H-19 and the steel core is galvanized, of class A, B, or C.

Code names and properties of different ACSR cables are summarized in Table 3.5. A cable designated as X/Y means that it has X aluminum strands surrounding Y steel strands.

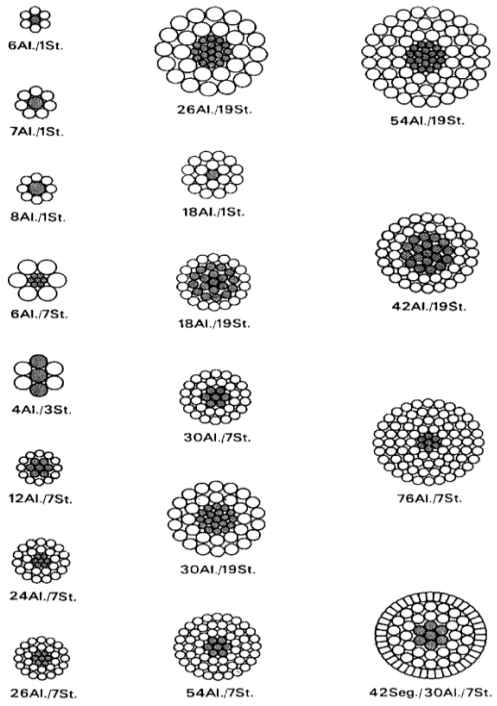

Figure 3.7: ACSR Construction[15]

[15] *http://electrical-engineering-portal.com/conductor-types-used-for-overhead-lines* [Last accessed on 01/31/2019]

Table 3.5: ACSR Cable Types and Properties (American Wire Group, 2018)

Code Name	Stranding (Al/Steel)	Diameter of Al Strand (in)	Diameter of Steel Strand (in)	Diameter of Steel Core (in)	Diameter of Complete Cable (in)	Al Weight (lb/MFT)	Steel Weight (lb/MFT)	Tensile Breaking Load (lb)
Joree	76/19	0.1819	0.0849	0.4245	1.88	2384	364.8	61700
Bluebird	84/19	0.1602	0.0961	0.4805	1.762	2044	467.4	60300
Thrasher	76/19	0.1744	0.0814	0.407	1.802	2191	335.4	56700
Falcon	54/19	0.1716	0.103	0.515	1.545	1507	537	54500
Parrot	54/19	0.1672	0.1003	0.5015	1.505	1431	509.2	51700
Chukar	84/19	0.1456	0.0874	0.437	1.602	1688	386.6	51000
Kiwi	72/7	0.1735	0.1157	0.3471	1.735	2055	248.9	49800
Plover	54/19	0.1628	0.0977	0.4885	1.465	1357	483.1	49100
Martin	54/19	0.1582	0.9049	0.4745	1.424	1281	455.8	46300
Pheasant	54/19	0.1535	0.0921	0.4605	1.382	1206	429.3	43500
Lapwing	45/7	0.1880	0.1253	0.3759	1.504	1498	292.2	42200
Grackle	54/19	0.1486	0.0892	0.446	1.338	1130	402.7	41900
Nuthatch	45/7	0.1832	0.1221	0.3663	1.465	1425	277.4	40100
Finch	54/19	0.1436	0.0862	0.431	1.293	1056	276.1	39100
Mallard	30/19	0.1628	0.0977	0.4885	1.14	751.9	483.1	38400
Bobolink	45/7	0.1783	0.1189	0.3567	1.427	1350	263.1	38300
Curlew	54/7	0.1383	0.1383	0.4149	1.245	974.3	355.6	36600
Dipper	45/7	0.1733	0.1155	0.3465	1.386	1275	248.3	36200
Redwing	30/19	0.1544	0.0926	0.463	1.081	676.3	434	34600
Bittern	45/7	0.1681	0.1121	0.3363	1.345	1200	233.9	34100
Cardinal	54/7	0.1329	0.1329	0.3987	1.196	900.7	328.4	33800
Bunting	45/7	0.1628	0.1085	0.3255	1.302	1125	219.1	32000
Canary	54/7	0.1291	0.1291	0.3873	1.162	849	309.9	31900
Egret	30/19	0.1456	0.0874	0.437	1.019	601.4	386.6	31500
Drake	26/7	0.1749	0.136	0.408	1.108	750.3	344.2	31500
Scoter	30/7	0.1456	0.1456	0.4368	1.019	601.4	394.9	30400
Teal	30/19	0.1420	0.0852	0.426	0.994	572	367.4	30000
Bluejay	45/7	0.1573	0.1049	0.3147	1.259	1050	204.8	29800
Wood-Duck	30/7	0.1420	0.142	0.426	0.994	572	375.6	28900
Starling	26/7	0.1659	0.129	0.387	1.051	675	309.7	28400
Condor	54/7	0.1213	0.1213	0.3639	1.092	749.5	273.6	28200
Cuckoo	24/7	0.1820	0.1213	0.364	1.092	749.9	273.8	27900
Eagle	30/7	0.1362	0.1362	0.4086	0.953	526.3	345.6	27800
Ortolan	45/7	0.1515	0.101	0.303	1.212	974.3	189.8	27700
Gannet	26/7	0.1601	0.1245	0.373	1.014	628.7	288.5	26400
Rail	45/7	0.1456	0.0971	0.2913	1.165	899.9	175.5	25900
Stilt	24/7	0.1727	0.1151	0.3453	1.036	675.2	246.5	25500
Grosbeak	26/7	0.1564	0.1216	0.3648	0.99	597.9	276.2	25200
Ruddy	45/7	0.1414	0.0943	0.2829	1.131	848.7	165.5	24400
Squab	26/7	0.1525	0.1186	0.3558	0.966	570.4	261.8	24300
Hen	30/7	0.1261	0.1261	0.3783	0.883	451.1	296.2	23800
Flamingo	24/7	0.1667	0.111	0.333	1	629.1	229.7	23700
Rook	24/7	0.1628	0.1085	0.3255	0.977	600	219.1	22600
Dove	26/7	0.1463	0.1138	0.3414	0.927	525	241	22500
Tern	45/7	0.1329	0.0886	0.2548	1.063	749.8	146.1	22100
Peacock	24/7	0.1588	0.1059	0.3177	0.953	570.9	208.7	21600
Lark	30/7	0.1151	0.1151	0.3453	0.806	375.8	246.8	20300
Parakeet	24/7	0.1523	0.1015	0.3045	0.914	525.1	191.7	19800

Hawk	26/7	0.1354	0.1053	0.3159	0.858	449.6	206.4	19500
Oriole	30/7	0.1059	0.1059	0.3117	0.741	318.2	208.9	17800
Flicker	24/7	0.1410	0.094	0.282	0.846	450.1	164.4	17200
Coot	36/1	0.1486	0.1486	0.1486	1.04	746.2	58.5	16800
Ibis	26/7	0.1236	0.0961	0.2882	0.783	374.7	171.9	16300
Kingbird	18/1	0.1880	0.188	0.188	0.94	597.2	93.6	15700
Brant	24/7	0.1287	0.0858	0.2574	0.772	375	137	14500
Linnet	26/7	0.1137	0.0884	0.2642	0.72	317.1	145.4	14100
Swift	36/1	0.1329	0.1329	0.1329	0.93	596.9	46.8	13800
Osprey	18/1	0.1758	0.1758	0.1758	0.879	522.2	81.8	13700
Ostrich	26/7	0.1074	0.0835	0.2505	0.68	282.9	129.8	12700
Pelican	18/1	0.1628	0.1628	0.1628	0.814	447.8	70.2	11800
Partridge	26/7	0.1013	0.0788	0.2364	0.642	251.7	115.6	11300
Chickadee	18/1	0.1486	0.1486	0.1486	0.743	373.1	58.5	9940
Merlin	18/1	0.1367	0.1367	0.1367	0.683	315.8	49.5	8680
Penguin	6/1	0.1878	0.1878	0.1878	0.563	197.7	93.4	8350
Waxwing	18/1	0.1217	0.1217	0.1217	0.609	250.3	39.2	6880
Pigeon	6/1	0.1672	0.1672	0.1672	0.502	156.7	74	6620
Quail	6/1	0.1489	0.1489	0.1489	0.447	124.3	58.7	5300
Raven	6/1	0.1327	0.1327	0.1327	0.398	98.7	46.6	4380
Sparate	7/1	0.0974	0.1299	0.1299	0.325	62	44.7	3640
Robin	6/1	0.1181	0.1181	0.1181	0.354	78.2	36.9	3550
Sparrow	6/1	0.1052	0.1052	0.1052	0.316	62	29.3	2850
Swanate	7/1	0.0772	0.1029	0.1029	0.257	39	28	2360
Swan	6/1	0.0834	0.0834	0.0834	0.25	39	18.4	1860
Turkey	6/1	0.0661	0.0661	0.0661	0.198	24.5	11.6	1190

3.4.2 All Aluminum Alloy Conductor (AAAC)

In an AAAC cable, standard 6201-T81 aluminum alloy is used instead of 1350-H-19. A higher strength-to-weight ratio is achieved using the former alloy, which improves the sag characteristics of AAACs. An AAAC cable does not have central steel core but has 6201-T81 aluminum alloy strands organized in a concentric-lay, as shown in Figure 3.8. An AAAC cable has higher corrosion resistance and greater resistance to abrasion than an ACSR cable. Table 3.6 summarizes some AAAC cable types and properties.

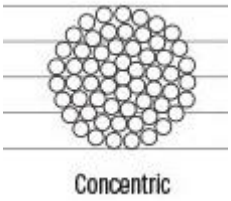

Figure 3.8: Concentric-Lay Cross-Section[16]

[16] https://www.anixter.com/es_la/resources/literature/wire-wisdom/american-wire-gauge.html [Last accessed on 01/31/2019]

Table 3.6: AAAC Cable Types and Properties (Priority Wire & Cable, 2016)

Code Name	Stranding (Al)	Diameter of Each Strand (in)	Diameter of Complete Cable (in)	Cross Sectional Area (in^2)	Steel Weight (lb/MFT)	Tensile Breaking Load (lb)
Greely	37	0.1583	1.108	0.7282	870.4	30500
Flint	37	0.1415	0.991	0.5818	695.5	24400
Elgin	19	0.1853	0.927	0.5124	612.4	21900
Darien	19	0.1716	0.858	0.4394	525.2	18800
Cairo	19	0.1565	0.783	0.3655	436.9	15600
Canton	19	0.1441	0.721	0.3098	370.3	13300
Butte	19	0.1283	0.642	0.2456	293.6	11000
Alliance	7	0.1878	0.563	0.1939	231.8	8560
Amherst	7	0.1672	0.502	0.1537	183.7	6790
Anaheim	7	0.1490	0.447	0.1221	145.9	5390
Azusa	7	0.1327	0.398	0.0968	115.7	4460
Ames	7	0.1052	0.316	0.0608	72.7	2800
Alton	7	0.0834	0.250	0.0382	45.7	1760
Akron	7	0.0661	0.198	0.0240	28.7	1110

3.4.3 Aluminum Conductor Alloy Reinforced (ACAR)

The core in an ACAR cable is made of 6201-T81 aluminum alloy wires, wrapped around by 1350-H-19 aluminum wires. This construction provides a good weight-to-strength ratio compared to an ACSR cable. An ACAR cable also has a very good resistance to corrosion. Table 3.7 summarizes some ACAR cable types and properties.

Table 3.7: ACAR Cable Types and Properties (American Wire Group, 2018)

Name	Stranding (Al 1350/Al 6201)	Diameter of 6201 Strand (in)	Diameter of 1350 strand (in)	Diameter of Complete Cable (in)	Weight (lb/MFT)	Tensile Breaking Load (lb)
ACAR-2493.0	54/37	0.1655	0.1655	1.821	2354.5	57600
ACAR-2493.0	72/19	0.1655	0.1655	1.821	2356.9	50400
ACAR-2267.0	42/19	0.1928	0.1928	1.735	2142	49900
ACAR-1933.0	42/19	0.1780	0.178	1.602	1808.8	42500
ACAR-1703.0	42/19	0.1671	0.1671	1.504	1593.5	37500
ACAR-1527.0	42/19	0.1582	0.1582	1.424	1428.8	33600
ACAR-1280.0	18/19	0.1860	0.186	1.302	1196.5	32200
ACAR-1361.0	42/19	0.1494	0.1494	1.344	1273.6	30300
ACAR-1197.0	18/19	0.1799	0.1799	1.259	1118.9	30200
ACAR-1172.0	18/19	0.1780	0.178	1.246	1095.5	29500
ACAR-1109.0	18/19	0.1731	0.1731	1.212	1036.6	27900
ACAR-1081.0	18/19	0.1709	0.1709	1.196	1010.5	27200
ACAR-1280.0	30/7	0.1860	0.186	1.302	1198.5	26200
ACAR-1024.5	18/19	0.1664	0.1664	1.165	957.7	25800
ACAR-1197.0	30/7	0.1799	0.1799	1.259	1120.8	24500
ACAR-1172.0	30/7	0.1780	0.178	1.246	1097.3	24000
ACAR-927.2	18/19	0.1583	0.1583	1.108	866.7	23400
ACAR-1109.0	30/7	0.1731	0.1731	1.212	1038.4	22700

ACAR-1081.0	30/7	0.1709	0.1709	1.196	1012.1	22100
ACAR-853.7	18/19	0.1519	0.1519	1.063	798	21500
ACAR-1024.5	30/7	0.1664	0.1664	1.165	959.3	20900
ACAR-927.2	30/7	0.1583	0.1583	1.108	868.2	19000
ACAR-739.8	18/19	0.1414	0.1414	0.99	691.6	18800
ACAR-853.7	30/7	0.1519	0.1519	1.063	799.3	17500
ACAR-653.1	12/7	0.1854	0.1854	0.927	611	15400
ACAR-739.8	30/7	0.1414	0.1414	0.99	692.7	15300
ACAR-503.6	12/7	0.1628	0.1628	0.814	471.1	11900
ACAR-465.9	12/7	0.1566	0.1566	0.783	435.8	11000
ACAR-355.0	12/7	0.1367	0.1367	0.683	332.1	8500

Nomenclature:
ACAR – 2493 means that the cross-sectional area is 2493 kcmil.
1 kcmil = 0.507 mm^2 = 0.0007858 in^2

3.4.4 Trapezoidal Aluminum Alloy Conductor Steel Reinforced (ACSR/TW)

Aluminum strands in the ACSR/TW cable are trapezoidal in shape to allow for a more compact alignment around the steel core. The wedge-like construction reduces the space occupied by air and gives the same cross-sectional area by reducing the overall diameter of the cable. Outer strands are made of aluminum 1350-H-19, and galvanized steel of different classes may be used in the core. The reduced size of the cable diminishes the effect of ice and wind loads. Figure 3.9 shows the construction of an ACSR/TW cable, and Table 3.8 summarizes some ACSR/TW cable types and properties.

Figure 3.9: ACSR/TW Construction[17]

Table 3.8: ACSR/TW Cable Type and Properties (American Wire Group, 2018)

Code Name	Conductor Area		Stranding			Outside Diameter		Weight (lb/MFT)			Tensile Breaking Load (lb)
	Al (in^2)	Total (in^2)	No. of Layers of Al	Al Strands	Steel Strands x Diameter (in)	Complete Conductor (in)	Steel Core (in)	Total	Al	Steel	
Santee/TW	2.0630	2.2268	4	64	19x0.1062	1.762	0.531	3048	2477	571	74500
Cumberland/TW	1.5134	1.7049	3	42	19x0.1133	1.545	0.5665	2471	1821	650	65300
Bluebird/TW	1.0934	1.8312	4	64	19x0.0961	1.608	0.4805	2515	2047	468	61100
Powder/TW	1.6912	1.8290	4	64	19x0.0961	1.602	0.4805	2498	2030	468	61100
James/TW	1.3590	1.5314	3	34	19x0.1075	1.47	0.5375	2221	1636	585	59400
Pecos/TW	1.2739	1.4429	3	39	19x0.1064	1.424	0.532	2107	1533	574	57500
Falcon/TW	1.2488	1.4071	3	42	19x0.1030	1.408	0.515	2040	1503	537	55100
Rio Grande/TW	1.2043	1.3571	3	39	19x0.1012	1.382	0.506	1968	1449	519	53200

[17] *http://www.cmewire.com/catalog/sec03-bac/bac-10-acsrtw.php* [Last accessed on 01/31/2019]

Athabaska/TW	1.5312	1.6377	3	44	7x0.1392	1.504	0.4176	2199	1838	361	51900
Chukar/TW	1.3986	1.5120	3	37	19x0.0874	1.445	0.437	2063	1676	387	50700
Merrimack/TW	1.1250	1.2677	3	39	19x0.0978	1.34	0.489	1840	1356	434	49700
Plover/TW	1.1239	1.2664	3	44	19x0.0977	1.337	0.4885	1836	1353	483	49600
Martin/TW	1.0615	1.1959	3	42	19x0.0949	1.3	0.4745	1734	1278	456	46800
Pee Dee/Tw	1.3810	1.4770	3	37	7x0.1319	1.427	0.3957	1982	1658	324	46700
Thames/TW	1.3480	1.1809	3	39	19x0.0944	1.29	0.472	1713	1261.6	451.4	46300
Pheasant/TW	0.9990	1.1256	3	39	19x0.9210	1.264	0.4605	1632	1202	430	44100
Schuylkill/TW	1.3020	1.3920	3	36	7x0.128	1.386	0.384	1868	1563	305	44000
Yukon/TW	0.9689	1.0925	3	38	19x0.0910	1.245	0.455	1586	1166.5	419.5	42900
Lapwing/TW	1.2488	1.3351	3	36	7x0.1253	1.358	0.3759	1791	1499	292	42200
Grackel/TW	0.9366	1.0554	3	38	19x0.0892	1.225	0.446	1530	1127	403	41900
Potomac/TW	1.2232	1.3079	3	36	7x0.1241	1.345	0.3723	1755	1468	287	41900
Hudson/TW	0.9098	1.0281	2	26	7x0.1467	1.196	0.4401	1489	1089	400	39600
Miramichi/TW	1.1430	1.2222	3	36	7x0.1200	1.302	0.36	1640	1372	268	39200
Finch/TW	0.8742	0.9851	3	38	19x0.0862	1.185	0.431	1429	1052.6	376.4	39100
Bobolink/TW	1.1236	1.2017	3	36	7x0.1189	1.291	0.3567	1613	1350	263	38900
Platte/TW	1.2323	1.2957	3	33	7x0.1074	1.334	0.3222	1693	1478	215	38200
Suwannee/TW	0.7537	0.8762	2	22	7x0.1493	1.108	0.4479	1318	903	415	37000
Mackenzie/TW	1.0679	1.1418	3	36	7x0.1559	1.259	0.3477	1530	1280	250	36900
Dipper/TW	1.0615	1.1348	3	35	7x0.1155	1.256	0.3465	1522	1274	248	36700
Curlew/TW	0.8117	0.9169	2	20	7x0.1383	1.129	0.4149	1327	971.1	355.9	36300
St. Croix/TW	1.1529	1.2124	3	33	7x0.1041	1.292	0.3123	1585	1383	202	35800
Bittern/TW	0.9990	1.0681	3	35	7x0.1121	1.22	0.3363	1433	1198	234	34600
Nelson/TW	0.9874	1.0557	3	35	7x0.1115	1.213	0.3345	1417	1185.7	231.3	34200
Columbia/TW	0.7589	0.8573	2	21	7x0.1338	1.092	0.4014	1241	908	333	34000
Cardinal/TW	0.7493	0.8464	2	20	7x0.1329	1.084	0.3987	1226	897.3	328.7	33500
Truckee/TW	1.0780	1.1334	3	30	7x0.1004	1.248	0.3012	1481	1293.4	187.6	33400
Bunting/TW	0.9366	1.0013	3	34	7x0.1085	1.181	0.3255	1343	1124	219	32400
Drake/TW	0.6244	0.7261	2	20	7x0.1360	1.01	0.408	1092	747.8	344.2	31800
Genesee/TW	0.9095	0.9733	3	33	7x0.1078	1.165	0.3234	1308	1092	216	31600
Scissortail/TW	0.9991	1.0505	3	30	7x0.0967	1.203	0.2901	1372	1198	174	31400
Catawba/TW	0.9991	1.0505	3	30	7x0.0967	1.203	0.2901	1372	1198	174	31400
Wabash/TW	0.5992	0.6966	2	20	7x0.1331	0.99	0.3993	1047	717	330	30500
Bluejay/TW	0.8742	0.9347	3	33	7x0.1049	1.143	0.3147	1257	1052.2	204.8	30300
Fraser/TW	0.7436	0.8168	3	35	7x0.1154	1.077	0.3462	1142	894	248	29600
Oxbird/TW	0.9366	0.9848	2	30	7x0.0936	1.167	0.2808	1286	1123	163	29500
Cheyenne/TW	0.9175	0.9646	3	30	7x0.0926	1.155	0.2778	1260	1100.4	159.6	28900
Condor/TW	0.6244	0.7053	2	20	7x0.1203	0.993	0.3639	1021	747.2	273.8	28200
Ortolan/TW	0.8117	0.8678	3	32	7x0.1010	1.102	0.303	1165	975.2	189.8	28100
Maumee/TW	0.6034	0.6819	2	20	7x0.1195	0.977	0.3585	987.8	722.1	265.7	27700
Avocet/TW	0.8742	0.9191	3	30	7x0.0904	1.129	0.2712	1201	1048.9	152.1	27500
Oswego/TW	0.5221	0.6072	2	20	7x0.1244	0.927	0.3732	913.4	625.4	288	26600
Kettle/TW	0.7518	0.8038	3	32	7x0.0973	1.06	0.2919	1079	902.8	176.2	26000
Puffin/TW	0.6244	0.6919	2	18	7x0.1108	0.98	0.3324	975.3	746.9	228.4	25900
Rail/TW	0.7493	0.8011	3	32	7x0.0971	1.061	0.2913	1075	900	175	25900
Snowbird/TW	0.8117	0.8534	3	30	7x0.0871	1.089	0.2613	1115	973.8	141.2	25700
Grosbeak/TW	0.4995	0.5808	2	20	7x0.1216	0.908	0.3648	873.5	598.4	275.1	25400
Mystic/TW	0.5236	0.5914	2	20	7x0.1111	0.913	0.333	856.3	626.6	229.7	24000
Phoenix/TW	0.7493	0.7876	3	30	7x0.0837	1.044	0.2511	1032	901.6	130.4	23700
Rook/TW	0.4995	0.5643	2	19	7x0.1085	0.89	0.3255	816	597.9	219.1	22900
Calumet/TW	0.4439	0.5165	2	18	7x0.1147	0.858	0.3438	714.8	523.1	191.7	22900
Dove/TW	0.4371	0.5083	2	20	7x0.1138	0.852	0.3414	764.5	523.5	241	22600

Tern/TW	0.6244	0.6675	2	17	7x0.0886	0.96	0.2658	892	745.9	146.1	21000
Mohawk/TW	0.4490	0.5074	2	18	7x0.1030	0.846	0.309	734.7	537.3	197.4	20700
Parakeet/TW	0.4371	0.4937	2	18	7x0.1015	0.835	0.3045	714.9	523.2	191.7	20000
Hawk/TW	0.3746	0.4356	2	18	7x0.1053	0.789	0.3159	655	448.7	206.3	19400
Flicker/TW	0.3747	0.4233	2	18	7x0.0940	0.776	0.282	612.8	448.4	164.4	17200
Nechako/TW	0.6039	0.6220	3	27	1x0.1520	0.93	0.152	781.9	720.7	61.2	16400
Swift/TW	0.4995	0.5133	3	27	1x0.1329	0.85	0.1329	646	599.2	46.8	13500
Monongahela/TW	0.3181	0.3362	2	14	1x0.1520	0.68	0.152	441	379.8	61.2	10200
Merlin/TW	0.2642	0.2788	2	14	1x0.1367	0.63	0.1367	365	315.5	49.5	8560

More information about different kinds of cables and their properties can be found in the following references: (The Aluminum Association, 1999), (Nexans, 2003), and (General Cable, 2017).

Observations from the data collected:

Largest Tensile Breaking Load: 142,800 lb
Alum-01, Diameter = 1.270 in

Largest Cable Diameter: 1.88 in
Joree (ACSR cable), Breaking load = 61,700 lb

4. WIRE STRIKE PREVENTION AND PROTECTION TECHNOLOGIES

As discussed earlier, most of the wire-strike accidents highlighted in the FAA study (Nagaraj & Chopra, 2008) could have been prevented if the pilot would have had a warning about the proximity of the helicopter to the wires, or if a protection device would have been installed on the helicopter. Several systems that may safeguard helicopters from wire strikes are available commercially and some of them are discussed in the following sections.

4.1 POWER LINE DETECTION SYSTEM (PDS)

Power lines are one of the primary hazards for low altitude operations. A system was developed by Safe Flight Instrument Corporation to detect active power lines close to a helicopter and to provide audio and visual warnings to the pilot. The electromagnetic field emitted by active power lines is detected by a sensor located at the front of the fuselage below the nose, as depicted in Figure 4.1. The sensor antennas are connected to a very low frequency band-pass filter which can detect frequencies around 60 Hz.

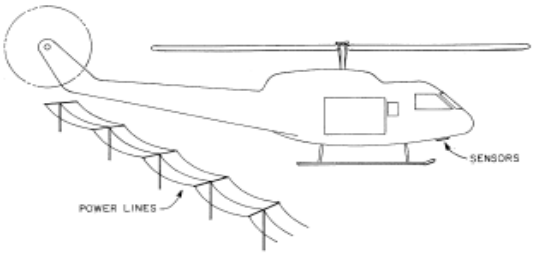

Figure 4.1: Schematics of Operation (Cornelio & Crocker, 1999)

The system, shown in Figure 4.2, weighs around 14 ounces (0.39 kg). It has a red "WARN" light, a yellow "MUTE" light, and a rotary sensitivity adjustor. When a power line is detected, the red "WARN" light lights up and a Geiger counter-like click sound is heard in the pilot's audio system. The frequency of the clicks changes according to the proximity of the power line and the speed at which the helicopter is approaching the power line. The pilot can choose to mute the audio output if required; However, the "WARN" light will remain on as long as the power line is detected. A sensitivity knob allows the pilot to dial out nuisance warnings.

Figure 4.2: Power line Detection System (PDS)[18]

Sensor antennas also can be placed at the aft end to detect wires behind the helicopter. Tests have shown that a DPS can detect a 22 kV power line located a mile away. The latest version of the PDS is called the DPDS (Dual Frequency PDS). It can detect frequencies of 60 Hz (in the U.S.), and 50 Hz (international). The DPDS is FAA certified and is being used on the Airbus SA 341,

[18] *http://aviationweek.com/business-aviation/flying-safe-flight-s-pds* [Last accessed on 01/31/2019]

the Gazelle, and the Bell 206. It is also certified by the European Aviation Safety Agency (EASA) and the Civil Aviation Safety Authority (CASA). It costs around $12,000.

Claims

- The PDS can detect active power lines as far as 1.5 km
- The PDS is tuned to detect electromagnetic waves only from power lines

Advantages

- Simple and lightweight system
- Can detect active power lines over long distances
- Easy Installation

Disadvantages

- Cannot detect power lines that are not active
- Cannot detect other types of wires, like guy wires or static wires

4.2 TERRAIN AWARENESS AND WARNING SYSTEM (TAWS)

The Terrain Awareness and Warning system (TAWS) was developed in the 1970s and was made mandatory in almost all planes to avoid accidents involving Controlled Flight Into Terrain (CFIT). The TAWS was invented by Honeywell engineer Don Bateman, who first developed the ground-proximity warning system, illustrated in Figure 4.3. The TAWS uses an on-board terrain database, displays 2-D information on a screen, and provides warning when the aircraft comes in proximity to the ground, water, or an obstacle. A typical TAWS system is shown in Figure 4.4.

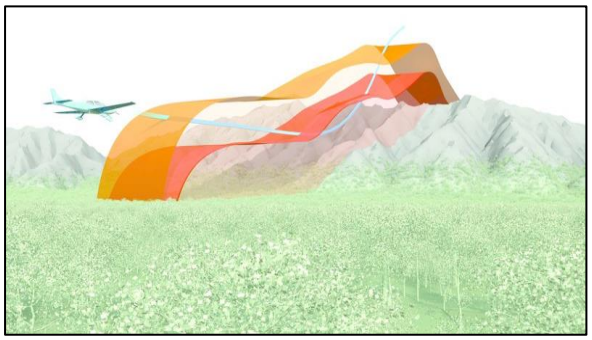

Figure 4.3: An Illustration of TAWS Working Principle[19]

Figure 4.4: Garmin GMX-200 Screen[20]

The TAWS uses aircraft altitude, position, and velocity data from flight instruments and GPS, and superimposes the plane's position with the the Earth's terrain and obstacles.
The terrain information displayed on the screen is color coded with respect to the aircraft current altitude as follows:

- Red: above 2000 feet
- Yellow: above 1000-2000 feet
- Light yellow: below 500 feet & above 1000 feet

[19] *https://www.flyingmag.com/how-it-works-terrain-awareness-and-warning-system* [Last accessed on 01/31/2019]
[20] *https://buy.garmin.com/en-US/US/p/6422* [Last accessed on 01/31/2019]

- Dark green: below 500-1000 feet
- Light green: below 1000-2000 feet
- Black: below 2000 feet

If the aircraft is flying into a yellow or a red region, hard warnings are given to the pilot to pull up or change course. Terrain awareness and warning systems has been modified for helicopters, and databases of transmission lines and other obstacles have been added. Some of the well-known terrain awareness and warning systems for helicopters are Garmin's Helicopter TAWS (HTWAS) and Sandel's ST3400H HeliTAWS, displayed in Figure 4.5 and Figure 4.6, respectively.

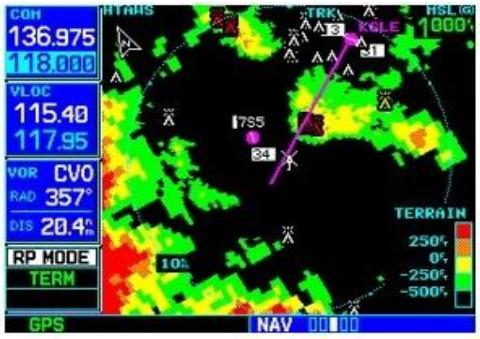

Figure 4.5: Garmin's HTAWS[21]

Figure 4.6: Sandel's HeliTAWS[22]

The Garmin system has WireAware, which is a database of power lines in the U.S. and some locations in Canada and Mexico. Power line information is displayed on the screen along with terrain information, and warnings are given in case of an impending collision with a transmission line. Sandel's WireWatch serves as the wire-lines database in HeliTAWS. HeliTAWS claims to have fewer nuisance alerts due to the TruAlert technology, an algorithm in HeliTAWS that reduces false alerts.

Claims

- Garmin's WireAware: most comprehensive wire database
- Sandel's TruAlert: optimized to remove false alerts

Advantages

- Systems give information about natural and man-made obstacles
- Visual system provides better situational awareness

Disadvantages

- Costly equipment (HTWAS - $35,000, HeliTAWS - $22,500)
- Accuracy of information depends on accuracy of databases
- False warnings could distract pilot

[21] *https://buy.garmin.com/en-US/US/p/72799* [Last accessed on 01/31/2019]
[22] *http://www.sandel.com/sandel-avionics-products/item/helicopter/st3400h-helitaws-3-ati-terrain-safety-system-3* [Last accessed on 01/31/2019]

4.3 WIRE CUTTERS

Wire-cutter systems are designed to protect helicopters in case of a wire strike. The most common and commercially available wire-cutter system is manufactured by Bristol Aerospace Limited (BAL) in Winnipeg, Canada, a subsidiary of the Magellan Aerospace Company. BAL's wire-cutter system is called Wire Strike Protection System (WSPS). It was developed for KIOWA (OH-58) helicopters in 1979.

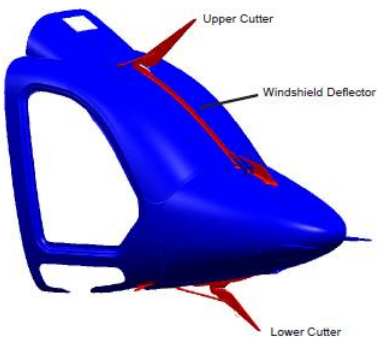

(a): Overview of the WSPS System[23]

(b): WSPS Cutter[24]

Figure 4.7: WSPS System

The system has two wire cutters with cutting blades made of hardened steel. The blades are located at the front end of fuselage, above the wind shield, and below the nose, as shown in Figure 4.7 (a). The system also has a deflector, attached to the center of the windshield, that deflects into the upper cutter any wire that strikes the windshield.. Some deflectors also have a serrated edge to damage and weaken the wire before it reaches the upper cutter. The wire cutters have extended arms that deflect wires into the cutters, should the wires be in a position to hit the rotor mast or skid, as depicted in Figure 4.7 (b). The cutting blades are arranged in a "V" shape, facing forward, and the blades sever the wire by making a notch in the wire as it passes into the cutter. This is a passive system.

The WSPS for the OH-58 was designed to sever a 3/8-inch diameter, seven-strand cable with a tensile breaking strength of slightly above 10,000 pounds. This cable was found to be the cause of many fatal accidents.

The WSPS has been tested by BAL on the KIOWA helicopter and by the U.S. Army on the UH-1 helicopter. The U.S. Army conducted swing tests at the Impact Dynamics Research Facility, VA. The tests revealed that, for an impact speed of 40 knots and impact angles (angle between the cable and the helicopter flight path) greater than 60 degrees, the cutter was able to sever the cables successfully (Burrows L. T., 1982). Modifications have been made to the original design to accommodate different helicopter models.

The WSPS is manufactured for the following helicopter companies:

[23] *http://www.helicopterpage.com/html/unique.html* [Last accessed on 01/31/2019]
[24] *http://helimart.com/products/magellan.html* [Last accessed on 01/31/2019]

- Airbus Helicopters
- Bell Helicopters
- MD Helicopters
- Finnmeccanica
- Sikorsky
- Boeing
- Kawasaki
- Kazan
- Kamov
- Hindustan Aeronautics Ltd
- Robinson Helicopters

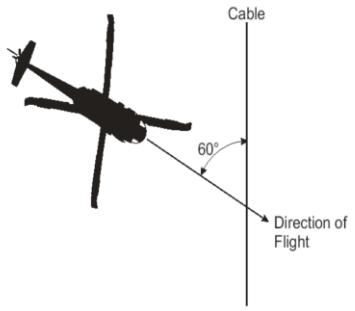

Figure 4.8: Minimum Strike Angle (Nagaraj & Chopra, 2008)

Although the WSPS covers a significant portion of the helicopter frontal area, it does not cover all of it. The coverage depends on the helicopter model and its orientation during impact. Wire-strike protection systems are effective for helicopter speeds greater than 30 knots and impact angles greater than 60 degrees, as shown in Figure 4.8. For values below those, the system may not cut the wire (Nagaraj & Chopra, 2008). To overcome these deficiencies, active cutter systems have been proposed (McKown, 1989). The design of an active wire-cutter system would feature a mechanism to actively sever a wire if it entered the cutter. Although this is a promising technology, no active wire cutters currently exist on the market.

Claims

- WSPS can sever cables up to 3/8 inch diameter with a tensile strength of 10,000 pounds
- Operating range: speed greater than15 mph, yaw angle between 0 and 45 degrees

Advantages of WSPS

- Passive System
- Protects helicopter from an inevitable strike
- Lightweight system protects rotor and windshield

Disadvantages of WSPS

- Does not cover the whole helicopter frontal area
- Performance depends on speed and orientation of helicopter during strike
- Can be costly ($6,870 - $59,400 or more)
- Installation can be complicated
- Larger wires may not be severed

4.4 OBSTACLE AVOIDANCE AND WARNING SYSTEM (OAWS)

Obstacle avoidance systems scan for obstacles around a helicopter using radio waves or laser technologies and warn pilots if an obstacle is detected. These systems do not need a database to operate, hence can be used in uncharted regions. Laser technology is superior to radio waves as lasers can detect small objects and produce a precise image due to the short wavelengths of light. This technology is known as Light Imaging Detection and Ranging (LIDAR). Some LIDAR systems are discussed in the following sections.

4.4.1 Laser Obstacle Avoidance System (LOAM)

LOAM is a laser-based system developed by Leonardo Airborne and Space Systems. Lasers enable more accurate mapping of the environment than is possible with radio frequency systems. LOAM uses an eye-safe 1.55μm Erbium laser that can detect obstacles in the path of the helicopter. The field of view (FOV) of LOAM is shown in Figure 4.9.

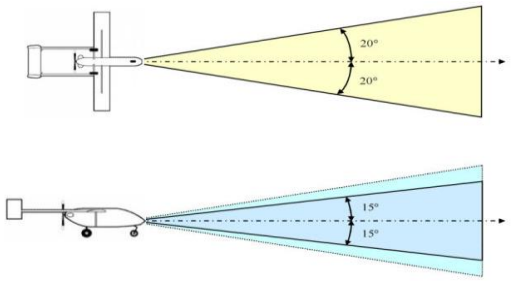

Figure 4.9: LOAM Field of View (Sabatini, Gardi, & Richardson, 2014)

The field of view can be changed ±20 degrees in both azimuth and elevation by moving the central optical axis, depending on the maneuver. LOAM scan rate is 4 Hz. During each scan, the laser traces the path shown in Figure 4.10. This elliptical pattern, known as a Palmer scan, covers most of the volume inside the FOV and can efficiently detect very thin obstacles.

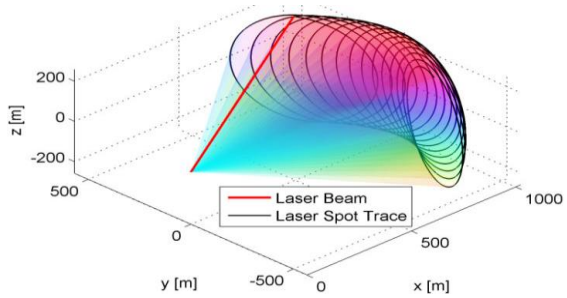

Figure 4.10: Laser Scan Pattern (Sabatini, Gardi, & Richardson, 2014)

The software used by the LOAM system picks up the data from the Palmer Scan, identifies obstacles, and provides information and warnings to the crew. The system has three components: a sensor head unit, a control panel, and a warning unit. The pilot can give commands to the LOAM unit using the control panel. The warning unit provides information about obstacles and suggests evasive maneuvers on a Multi-Function Display (MFD). The LOAM system is installed on the EH 101 and flight tested on the UH-101, Lynx, AB-212, and EC-130. A LOAM system installed on an AB-212 is shown in Figure 4.11.

Figure 4.11: LOAM System on AB-212 (Sabatini, Gardi, & Richardson, 2014)

4.4.2 Helicopter Laser Radar (HELLAS)

HELLAS is a laser-based system developed by Dornier GmbH. It is also based on the 1.5μm Erbium eye-safe laser. The HELLAS system is mounted under the fuselage and is connected to the helicopter navigation and intercom systems. The optical head of the HELLAS scans in the horizontal and vertical directions using a fiber-optical scanner and an oscillating-mirror, respectively. The scan pattern is not elliptical or circular like in a Palmer scan, but is a series of horizontal and vertical lines. This scan pattern has greater coverage within the FOV than a Palmer scan. The scan system produces a three-dimensional image of obstacles around the helicopter and can detect wires with a probability greater than 99.5% within one second of scanning the area.

The imaging feature of HELLAS makes it possible to use it as a navigational aid during poor-visibility conditions. The real-time scan display, shown in Figure 4.12, can be used to fly the helicopter at night and in inclement weather. The detection range of HELLAS varies from 300 m to 1000 m, depending on visibility and the sizes of the obstacles. The scan rate of HELLAS is 2 Hz. The software used in HELLAS is optimized to remove false warnings.

The HELLAS system has been tested on the CH53, UH1D, BK-117, EC-135 and EC-145. Dornier has installed the system on Germany's border-police helicopter fleet. A HELLAS system integrated into a EC-135 helicopter is shown in Figure 4.13.

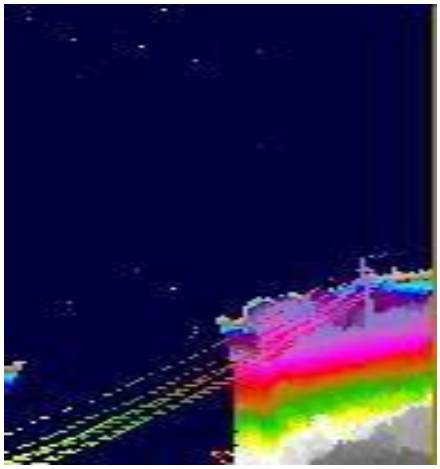

Figure 4.12: Wire-lines Scanned by HELL/ (Schulz, Scherbarth, & Fabry, 2002)

(a) **(b)**

Figure 4.13: HELLAS on EC 135 (Schulz, Scherbarth, & Fabry, 2002)

Claims

LOAM

- Detects 5 mm cable from a distance of 620 m in a 10 km visible range and from a distance of 500 m in a 1 km visible range
- Detection range of 2 km for large obstacles

HELLAS

- Detects 10 mm cable from a distance of 500 m in a 5 km visible range and from a distance of 300 m in a 1 km visible range
- Detection range of 1 km for large obstacles
- Detection probability of 99.5% for cables

Advantages of obstacle-avoidance systems

- Active systems
- Do not require a database
- Can detect thin obstacles like wires

Disadvantages of obstacle-avoidance systems

- Detection depends on field of view and weather conditions
- Heavyweight systems (~30 kg)
- Cost is very high (LOAM and HELLAS each cost approximately $100,000 (Nagaraj & Chopra, 2008))

4.5 WIRE/AERIAL MARKERS

Wire markers are probably the cheapest and simplest way to prevent wire strikes. Aerial markers, also known as overhead wire markers, aim to prevent wire strikes by making the wires more visible to aircraft flying at low altitudes. A typical wire marker is shown in Figure 4.14. Spherical markers are hollow spheres made of two halves. Figure 4.15 shows the bottom half attached to a wire with bushings at the points of contact. The top half is bolted to the bottom half, clamping down on the bushings to avoid slipping. The clamps are made of either aluminum or steel alloy.

Figure 4.14: Spherical Aerial Marker on a Wire[25]

Figure 4.15: Bottom Half of Spherical Aerial Marker[26]

The markers are made of fiber-reinforced plastic (FRP) with UV-resistant pigment to prevent color degradation that occurs due to long exposure to sunlight. FRP reduces the weight of the sphere significantly. Overhead markers are installed by utility companies to protect infrastructure from aircraft. The installation process is depicted in Figure 4.16. Markers come in various colors. International orange (#FF4F00) is the most-common color used in the aerospace industry to identify obstacles. Apart from orange, white and yellow are also used in some situations. An alternating pattern of orange, yellow, and white, as shown in Figure 4.17, is recommended by the FAA.

Figure 4.16: Installing Markers on Power lines[27]

Figure 4.17: Alternating Color Pattern[28]

Claims

- UV resistant pigment prevents color degradation
- 1.2 km visibility in all directions

Advantages

- Low cost ($100 to $200 per marker, popular manufacturer: TANA)
- Passive system
- No installation on helicopter necessary

Disadvantages

- Could be hard to see the markers in low light
- Marking every power line could be an arduous task
- Marker color could degrade over time
- Multiple markers required for a single catenary, cost could add up rapidly

[25] *https://flightlight.com/products/aerial-marker-balls-for-power-lines-model-jx/* [Last accessed on 01/31/2019]
[26] *http://www.poweng.com.au/power line markers.htm* [Last accessed on 01/31/2019]
[27] *http://aerossurance.com/helicopters/fatal-h500-hv-accident/* [Last accessed on 01/31/2019]
[28] *https://hillermuseum.wordpress.com/2010/05/28/helicopter-%E2%80%93-live-power-line-operations/* [Last accessed on 01/31/2019]

4.6 OBSTACLE COLLISION AVOIDANCE SYSTEM (OCAS)

OCAS, now known as Vestas InteliLight, is a system mounted on an obstacle on the ground. warns pilots when they areon a collision course with the obstacle. The system was developed in Norway and designed to operate in remote locations with low visibility and minimal power requirements.

OCAS has a radar unit, attached or placed close to the obstacle, that detects and tracks aircraft flying in the vicinity, as shown in Figure 4.18. The radar unit is connected to a light system that can provides a visual warning and/or illuminate the obstacle, as depicted in Figure 4.19. If an aircraft is in danger of striking the obstacle, the OCAS system activates the light system as a first warning, as shown in Figure 4.20.

Figure 4.18: OCAS Radar Unit[29]

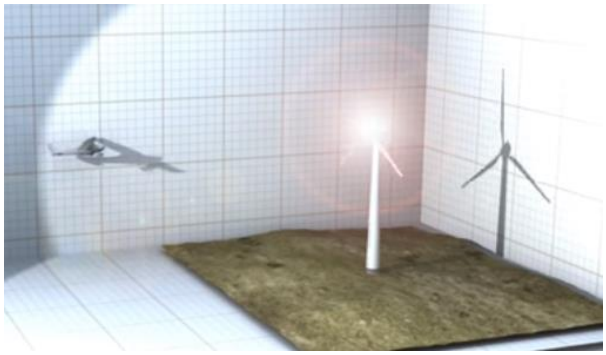

Figure 4.19: Visual Warning Light Turned ON[30]

Figure 4.20: An OCAS System Illuminating a Wind Turbine Farm for a Helicopter[31]

In case the first warning does not deter the aircraft from its course, OCAS sends an audio signal in the VHF warning spectrum to the aircraft's onboard radio. Once the aircraft maneuvers out of the collision course, the OCAS lights are automatically turned off. The light and radar systems are connected to a power source and a backup battery, so the system is functional during power outages.

---

[29] *https://www.youtube.com/watch?v=dzFD3r-vd40* [Last accessed on 01/31/2019]
[30] *https://www.youtube.com/watch?v=dzFD3r-vd40* [Last accessed on 01/31/2019]
[31] *https://www.youtube.com/watch?v=dzFD3r-vd40* [Last accessed on 01/31/2019]

OCAS has a detection range of 5km. An advantage of this system is that the warning lights are off unless required. This reduces light pollution and minimizes nuisance to public. The system also operates continuously and no additional equipment is required on the aircraft. The radar unit saves information about the warnings issued, including the speed, position, and size of each aircraft that entered the warning zone. Data logs are transferred to the OCAS Control Center (OCC) via the internet and the OCC creates a database of all air traffic in the vicinity. OCAS is approved by the FAA and the International Dark Sky Association. It is being used in Norway, the U.S., Canada, and Germany. This system is desired for power lines and wind-turbine farms.

Claims

- Minimum range of 8 km and maximum range of 36 km
- 3D terrain maps are used to ensure efficient radar coverage

Advantages

- System is activated only when required
- Reduces light pollution
- No installation on helicopter necessary

Disadvantages

- Range limited by radar capability and other obstacles in the path
- Multiple radars required for 360^{o} view
- High Cost ($50,000 per unit)

4.7 COMPARISON TABLE

Table 4.1: Wire Strike Prevention and Protection Technologies Comparison

Wire Strike Prevention and Protection Technology Characteristics	PDS	TAWS + Wire Database	WSPS System	LOAM	HELLAS	Aerial Markers	OCAS
Detecting Active Power lines	✓	✓	NA	✓	✓	✓	NA
Detecting All Types of Cables		✓	NA	✓	✓	✓	NA
Database Required	NA	✓	NA				
Audio Warning	✓	✓		✓	✓		✓
Visual Warning	✓	✓		✓	✓	✓	✓
Active System	✓	✓		✓	✓		✓
Passive System			✓			✓	
Protection from Wire Strike			✓				
Weather-Dependent Performance				✓	✓		
Costs Less than $15,000	✓		✓ (Depends)			✓	
Installed on Helicopter	✓	✓	✓	✓	✓		
Ground-Based System						✓	✓

5. ELECTRONIC FLIGHT BAG (EFB) OPTIONS

Electronic Flight Bags (EFBs) are devices that replace the paper documents of traditional flight bags. They facilitate a variety of flight-management tasks for the flight crew. The FAA defines an EFB as an electronic display system intended primarily for cockpit/flight deck or cabin use. Traditional flight bags normally contain essential documents, such as navigational charts, data for take-off calculations, an aircraft-operating manual, check lists, aircraft-performance data, fuel calculations, and so on. EFBs contain all this information in a digital format. Traditional flight bags weigh 18 kg or more and are labor intensive to use. EFBs weigh between 0.5 to 2.2 kg. Some EFBs are commercial-off-the-shelf (COTS) devices, like iPads and laptops, running EFB software, while other EFBs have special-purpose hardware with an interface that is easy-to-use during flight. A few advantages of using EFBs include:

- Reduced onboard weight
- Reduced cost
- Increased efficiency (easy to update)
- Increased safety
- Reduced pilot workload

A few EFBs are discussed briefly in the following sections.

5.1 FLITEDECK PRO

The FliteDeck Pro software, shown in Figure 5.1, was developed by Jeppesen, a Boeing Subsidiary. The latest version is called FliteDeck Pro 3.0/9.0. Previous versions of the software were compatible with devices that run Windows 8.1 or above, like Panasonic Toughpad, Samsung Galaxy TabPro S, Surface 2 RT, Surface 3, Surface Pro 3, and Surface Pro 4; however, FliteDec Pro 9.0 is compatible only with touch-screen devices that run Windows 10, and Pro 3.0 is compatible only with iOS v10 and above. FliteDeck Pro can be downloaded and installed using an internet connection like any other software.

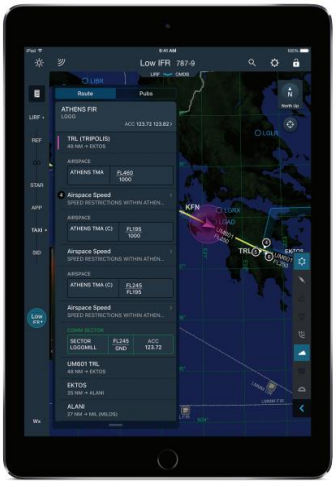

Figure 5.1: FliteDeck Pro Running on an iPad (Jeppesen, 2017)

FliteDeck Pro includes three main applications: enroute charts, terminal charts, and Airport Moving Map. The "enroute charts" application functions as a dynamic map that provides information to the pilot about the surrounding geography, weather, and flight route. It also displays navigational data, terrain contours, and allows pilots to modify their route if needed. Depending on the airspace an aircraft is flying in, local navigational guidelines are also displayed on the screen. The "terminal charts" application shows a static map of the origin or destination airport runways, terminals, and surrounding area. Notices to Airmen (NOTAMs) are displayed to warn pilots of any potential hazards along the flight route. The "Airport Moving Map" application features a detailed chart of the airport runways with the position of the aircraft on the ground, as depicted in Figure 5.2. It is provided as an aid to the pilot to increase situational awareness during taxi and after landing.

Figure 5.2: Airport Moving Map[32]

FliteDeck Pro features a "VFR-theme" option to display obstacles, including high-tension lines, suspended bridges, windmills, buildings, and towers. The coordinates of each obstacle, its height information, and the elevation of terrain at that location can be displayed on the screen by touching the obstacle icon. Jeppesen claims to have created the most comprehensive database of obstacles related to aviation.

5.2 T.BAGC2[2]

Manufactured by NavAero, t.BagC2[2], shown in Figure 5.3 and Figure 5.4, is an EFB with some parts integrated into the aircraft avionics. The EFB has a portable CPU that runs a relatively robust version of Windows XP. The display is a standard 8.4-inch color TFT LCD screen with resistive touch, and that is designed to be readable in sunlight. The portable CPU is connected to the aircraft power port and to data cables using certified connectors. The CPU case also has an emergency back-up battery.

Satellite communication devices can be connected to this EFB, using software designed by NavAero, for wireless connectivity. A video, surveillance system, called t-Cam, can be used to record cameras installed for cockpit and cargo monitoring. Any application designed for Windows XP and that performs real-time analysis of aircraft data can be installed on the t.BagC2[2]. An advantage of this EFB system is its modular design, every part can be upgraded separately. The system is designed to be cheap, easily maintainable, and to have a long life. It also offers communication with ground systems using additional devices.

[32] *http://ww1.jeppesen.com/aviation/products/airport-moving-maps/airport-moving-maps.jsp* [Last accessed on 01/31/2019]

Figure 5.3: t.BagC2[2] EFB System[33]

Figure 5.4: NavAero EFB Installed in a Cockpit[34]

5.3 AERA 660

Garmin's Aera 660 is a portable EFB that includes several features from Garmin's other products. Aera 660 is a tablet-like system shown in Figure 5.5. The system has a 5 inch capacitive touchscreen, which is sunlight readable, and built-in GPS and GLONASS. The screen can be used in either portrait or landscape mode. The Aera 660 is designed to be rugged, withstand high temperatures, and meet helicopter vibration standards. It has a mini USB port, a micro SD card slot, and a power button on the bezel.

Figure 5.5: Aera 660, Landscape and Portrait Mode[35]

A global terrain map, called 3D Vision, is included in the Aera 660and provides 3D elevation of terrain in the aircraft vicinity. Planned flight route, flight speed, altitude, and vertical speed are shown along with terrain information. Using wireless connectivity, Aera 660 can display weather, as shown in Figure 5.6, and air-traffic data on terrain maps. Additional devices, such as the GTX 345 and Flight Stream, are required for this and ADS-B traffic. Built-in Wi-Fi can be used to update maps and other database when connected to the internet.

A striking feature of the Aera 660 is the presence of WireAware from the HTAWS system, discussed in section 4.2 . WireAware superimposes power line data onto maps and provides audio and visual warnings during close operation. Mean sea-level (MSL) and above-ground-level

---

[33] *Flying Magazine, Page 96, May, 2005.*

[34] *https://www.aircraftspruce.eu/avionics/electronic-flight-bags/navaero-t-pad-800/navaero-tbagc2-efb-c2-system-8-4-display.html* [Last accessed on 01/31/2019]

[35] *https://newsline.kitplanes.com/2016/03/01/garmin-unveils-the-aera-660-next-generation-aviation-portable/#more-8116* [Last accessed on 01/31/2019]

(AGL) altitudes of power lines are both displayed to reduce ambiguity. Terminal procedural charts, fuel-price data, and departure and arrival procedures are available as an option.

Figure 5.6: Weather Data Displayed on Aera 660[36]

5.4 FOREFLIGHT MOBILE

ForeFlight Mobile was built by ForeFlight, headquartered in Houston, Texas. It is available for use on iPads and iPhones. The application has comprehensive aeronautical maps of the U.S. and most of the rest of world, as shown on Figure 5.7. Depending on the level of zoom, the information displayed on the map varies. Maps on ForeFlight include airspace details, airport diagrams, VOR (VHF Omni-Directional Range) details, and airway information. An example map is shown on Figure 5.8.

Figure 5.7: Airspace Illustration on ForeFlight[37]

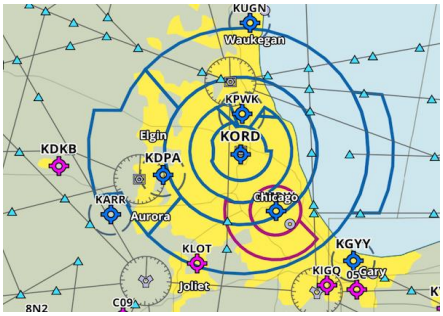

Figure 5.8: ForeFlight's Global Vector Aeronautical Map[38]

ForeFlight has a library of Visual Flight Rules (VFR) and Instrument Flight Rules (IFR) charts for the U.S. (including the Grand Canyon), Canada, the Caribbean, and the Gulf of Mexico. Metropolitan VFR charts for helicopter usage are also included in the map database. Terminal procedural maps, taxi charts, and current Temporary Flight Restrictions (TFR) maps are also available.

ForeFlight includes weather information received from either the internet or a special receiver installed onboard. Weather layers can be superimposed on the map to aid pilots in determining a safe flight path, and include turbulence data, pressure distribution charts, and, as shown in Figure 5.9, icing information.

---

[36] *https://newsline.kitplanes.com/2016/03/01/garmin-unveils-the-aera-660-next-generation-aviation-portable/#more-8116* [Last accessed on 01/31/2019]
[37] *https://www.foreflight.com/products/foreflight-mobile/maps/* [Last accessed on 01/31/2019]
[38] *https://www.foreflight.com/products/foreflight-mobile/* [Last accessed on 01/31/2019]

The hazard-avoidance feature of ForeFlight, called Hazard Advisor, uses the high-resolution terrain and obstacle database of Jeppesen. It combines this data with its own aeronautical maps to provide information about any obstacle that lies in the flight path, as shown in Figure 5.10. The aircraft GPS altitude is compared with the terrain elevation and the height of other obstacles. Warnings are provided in case some obstacles become a threat to the aircraft.

Figure 5.9: Icing Information Layer[39]

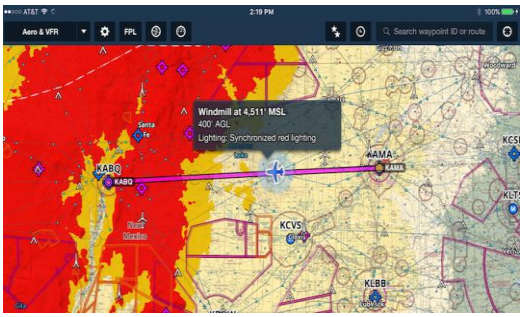

Figure 5.10: Hazard Advisor Warning[40]

5.5 FLYQ EFB 3.0

FlyQ is developed by Seattle Avionics and is designed to minimize the time spent looking at the EFB screen while flying. FlyQ is available on the Apple store for iPads and iPhones. FlyQ includes standard aeronautical maps in 2D format, 3D Synthetic Vision like Garmin, and Augmented Reality (AR) maps. 3D maps are generated using a terrain database that is stored in the system. 3D mode also displays roll and pitch status if an attitude and heading reference system (AHRS) is connected to FlyQ. Altitude and ground speed are shown besides the center box as shown in Figure 5.11.

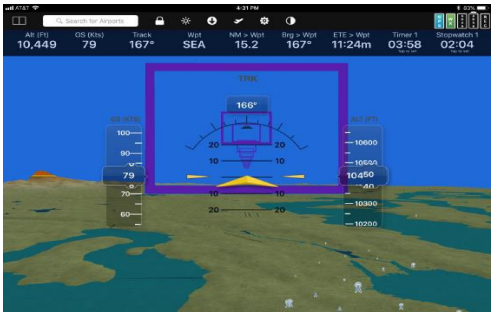

Figure 5.11: 3D Synthetic Vision (Seattle Avionics Software, 2018)

A unique feature of FlyQ is the presence of Augmented Reality maps. While in the AR mode, the pilot needs to point the iPad camera outside the window or windshield to have the closest airport displayed on the screen with a real-time view. The app uses GPS data and accelerometers to display and modify information as the aircraft is moving. This feature could prove to be convenient while flying in unfamiliar areas or during low-visibility conditions. The top half of Figure 5.12 shows an example of AR view. FlyQ also has an option to split the screen into two

[39] https://www.foreflight.com/products/foreflight-mobile/weather/ [Last accessed on 01/31/2019]
[40] https://www.foreflight.com/products/foreflight-mobile/hazard-avoidance/ [Last accessed on 01/31/2019]

halves, for displaying different applications, thus saving time while running two applications. Figure 5.12 shows the split-screen mode with AR and 2D maps displayed simultaneously.

FlyQ also has a flight-data recorder, which saves all information about a flight for subsequent review and analysis. Weather information is updated every eight minutes when an internet connection is available. As weather information is vital for flying, a color code is used to show the latest information to the pilot. Green is used if the weather map has been updated within the last sixty minutes, yellow if it was updated within four hours, and red if the last update was more than four hours ago. Air traffic surrounding the aircraft can also be displayed if an Automatic Dependent Surveillance-Broadcast (ADS-B) transponder is installed on the aircraft and connected to the FlyQ system. Weather data can be updated either from the internet or from the ADS-B system.

Figure 5.12: Split Screen with AR and 2D Maps[41]

A terrain and obstacle warning system is integrated into FlyQ. The pilot can choose to activate this system during low-altitude flight. The terrain is color coded, depending on the aircraft altitude and its velocity. For example, a red visual warning is triggered as the aircraft is heading towards an obstacle, as shown in Figure 5.13.

Figure 5.13: Obstacle Warning in FlyQ (Seattle Avionics Software, 2018)

5.6 HELIEFB

HeliEFB is EFB software specially designed for helicopters. It is available for use on iPads and desktop computers. HeliEFB focuses on flight-management tasks like weight and balance, flight-risk assessment, emergency checklists, and so on. HeliEFB is composed of three main modules:

- Weight & Balance and Performance
- Flight Risk Assessment (FRAT)
- Paperless Cockpit

[41] https://ipadpilotnews.com/2018/02/seattle-avionics-flyq-efb-3-0-adds-flight-recording-augmented-reality/ [Last accessed on 01/31/2019]

Helicopter weight and center of gravity are very sensitive to the distribution of passengers and/or cargo inside the fuselage due to its small size. These parameters have a great influence on helicopter control and performance. The Weight & Balance and Performance module allows for quick calculation of the performance of the helicopter based on the weight distribution inside the fuselage. A user can specify seating/cargo pods distribution and the weight of each passenger/cargo to get the performance data for the entire flight plan. Several helicopter models and seating-configuration data are integrated into the software, as shown in Figure 5.14.

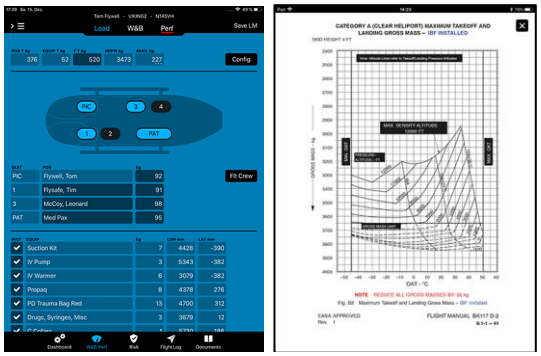

Figure 5.14: Seating Configuration and Performance Data in HeliEFB[42]

The FRAT module, shown in Figure 5.15, assesses flight risk based on a series of questions about an impending flight. FRAT provides a customized form to be filled out by crew members before departure. Based on the score assigned to each question, HeliEFB provides the risk associated with each flight. If the required score is not achieved or if certain requirements essential for a given flight are not satisfied, “no flight” will be recommended. The EFB is connected to an operations control center (OCC) for flight operations that require an operational approval. The FRAT module is FAA approved.

In the Paperless Cockpit Module displayed in Figure 5.16, all the documents required by the flight crew are available in a digital format. These documents include flight charts, manuals, operational checklists, emergency checklists, and medical centers with helipads. Documents can also be categorized based on the aircraft for easy access during search requests. Other documents can be uploaded onto the app and distributed to the entire fleet.

[42] https://heliefb.com/ [Last accessed on 01/31/2019]

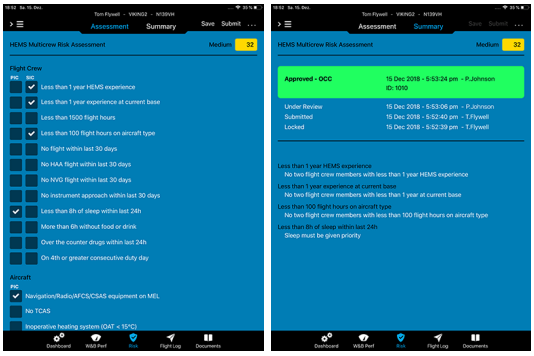

Figure 5.15: Flight Risk Assessment Module[43]

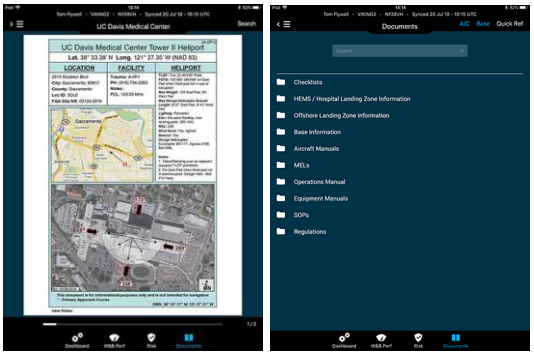

Figure 5.16: Paperless Cockpit Module[44]

5.7 RAMCO EFB

Ramco EFB is developed by Ramco Systems, headquartered in Chennai, India. This EFB not only includes flight management modules like weight and performance calculations, but also downstream processes like maintenance and billing. The modules provided by Ramco EFB include aircraft data, navigation, flight sheet, pilot/customer information, flight-log details, journey details, wind and temperature data, weight and balance calculation, and discrepancy and delay information, as shown in Figure 5.17.

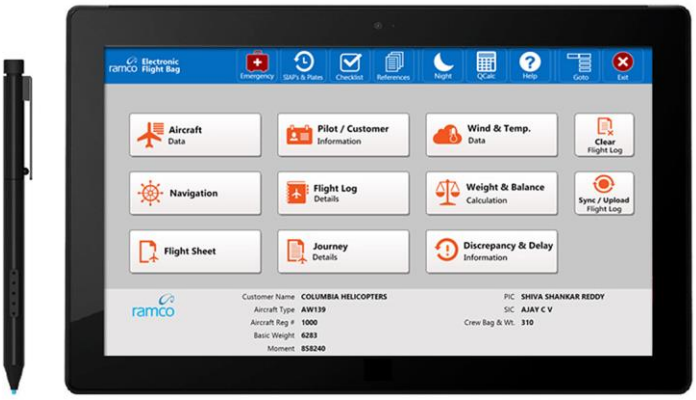

Figure 5.17: Ramco EFB Modules[45]

The presence of a stylus along with the tablet makes it easier to use during flight. The navigation module can be used to plan a flight path using aeronautical charts and route maps. Weight and balance calculations can be combined with navigation plans to determine the amount of fuel required for a given flight. Using the flight-sheet module, the Ramco EFB creates a document containing the time spent by the pilot and co-pilot in performing various flight tasks and the total time of the flight. The Ramco EFB also provides weather data using its wind and temperature module.

---

[43] https://heliefb.com/ [Last accessed on 01/31/2019]
[44] https://heliefb.com/ [Last accessed on 01/31/2019]
[45] http://www.ramco.com/aviation-suite/heli-operators/features-and-benefits/ [Last accessed on 01/31/2019]

All the essential documents, such as flight manuals, runway maps, and checklists are digitized and available for easy access at the top of the screen. A unique feature of the Ramco EFB is the integration of a Maintenance & Engineering (M&E) system. The EFB keeps track of the aircraft missions, the lengths of operations, and the maintenance parameters. This allows the operational crew to monitor the helicopter health and to perform maintenance when required. The software also acts as a log book by gathering real-time data about flight times, delays, and discrepancies. A billing module is included in the application to charge customers and generate invoices, thus reducing administration time and cost.

5.8 COMPARISON TABLE

Table 5.1: Electronic Flight Bags Comparison

EFBs / Features	FlightDeck Pro	t.BagC2[2]	Aera 660	ForeFlight Mobile	FlyQ EFB 3.0	HeliEFB	Ramco EFB
iOS	✓			✓	✓	✓	
Windows	✓	✓					
Other OS			✓				✓
Terrain Maps	✓	✓	✓	✓	✓		
Aeronautical Maps	✓	✓	✓	✓	✓	✓	✓
Dynamic Maps	✓	✓	✓	✓	✓		
Connection to Aircraft Avionics		✓					
Synthetic 3D Vision			✓	✓	✓		
Weather	✓	✓	✓	✓	✓		✓
Obstacle Avoidance	✓	✓	✓	✓	✓		
Augmented Reality					✓		
Split Screen					✓		
Flight Log		✓			✓		✓
Weight & Balance Calculations						✓	✓
Risk Assessment						✓	✓
Maintenance Data							✓

6. WIRE CUTTERS

6.1 PASSIVE WIRE CUTTERS

The Wire Strike Protection System (WSPS), described in section 4.3 , was originally designed by Nelson Chan to cut cables under tension. A U.S. Patent was assigned in 1980 (Chan, 1980) and it is currently the only commercially available wire cutter. The upper cutter of the WSPS is shown in Figure 6.1 (side view) and Figure 6.2 (front view).

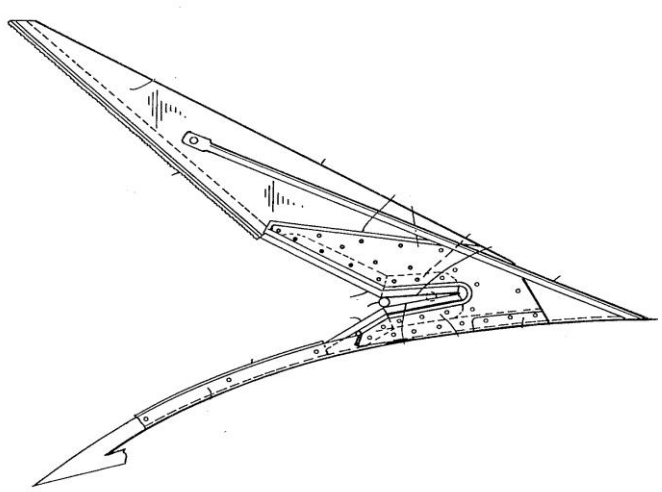

Figure 6.1: Side View of the Upper Cutter in the WSPS System (Chan, 1980)

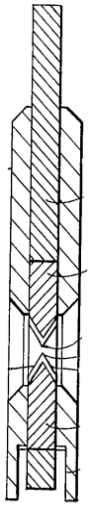

Figure 6.2: Front View of the Upper Cutter in the WSPS System (Chan, 1980)

Experience shows that about 80% of the time cable strikes occur in the helicopter nose region. The cable then proceeds over the windshield to the upper antenna, rotor mast, and rotor blades. In order to prevent the cable from reaching the rotor blades, the WSPS features a windshield deflector with a sharp edge so that the cable, after impacting the windshield, slides over the deflector into the cutter. In the WSPS, the upper and lower cutters have a wedge-like mechanism designed to partially cut cables so that they fail under tension. The cutting wedges are arranged at about 45^{o} apart and sever cables as they pass between the V-notch. As a cable starts to get severed and the tension starts to increase, stresses in the cable reach critical values and the cable tends to fail in tension before it fully traverses through the cutter. Hence, the performance of the cutter depends on the tension in the cable and the ability to create notches in the cable, which depends on the speed of the helicopter. Lower speeds could result in not enough tension to create a notch. Notch creation is a function of the knife-edge thickness of the cutter, material properties, and speed of impact.

Bristol Aerospace Limited (BAL) conducted tests on the upper cutter and the deflector installed on a KIOWA helicopter. The helicopter was fixed to the back of a truck on a flatbed and run into fixed wires. The speed of impact varied between 15 to 60 miles per hour and the impact angle ranged from 0 to 45 degrees. Steel-reinforced aluminum cables (10M) and guy cables were used during the test. The impact region was between the nose and the top of the upper cutter. According to Burrows (Burrows L. T., 1982), all these tests were successful in severing the

cables without causing any damage to the fuselage or affecting the flying qualities of the helicopter.

More detailed tests of the upper cutter, the deflection shield, and the lower cutter were conducted by the U.S. Army during the verification process of the WSPS for UH-1 helicopters. These tests addresssed issues such as:

1. Changes in pitch and yaw attitudes during the impact and severing process
2. Deceleration loads
3. Aircraft-handling properties
4. Windshield performance upon cable impact

Full-scale swing tests were conducted on the KIOWA and UH-1 helicopters at the Impact Dynamics Facility located in the Applied Technology Laboratory (ATL) of the U.S. Army Research and Technology Laboratories in Virginia (Burrows L. T., 1982), (Burrows L. T., 1980). The tests were conducted with a full-scale helicopter that may be swung like a pendulum, as shown in Figure 6.3.

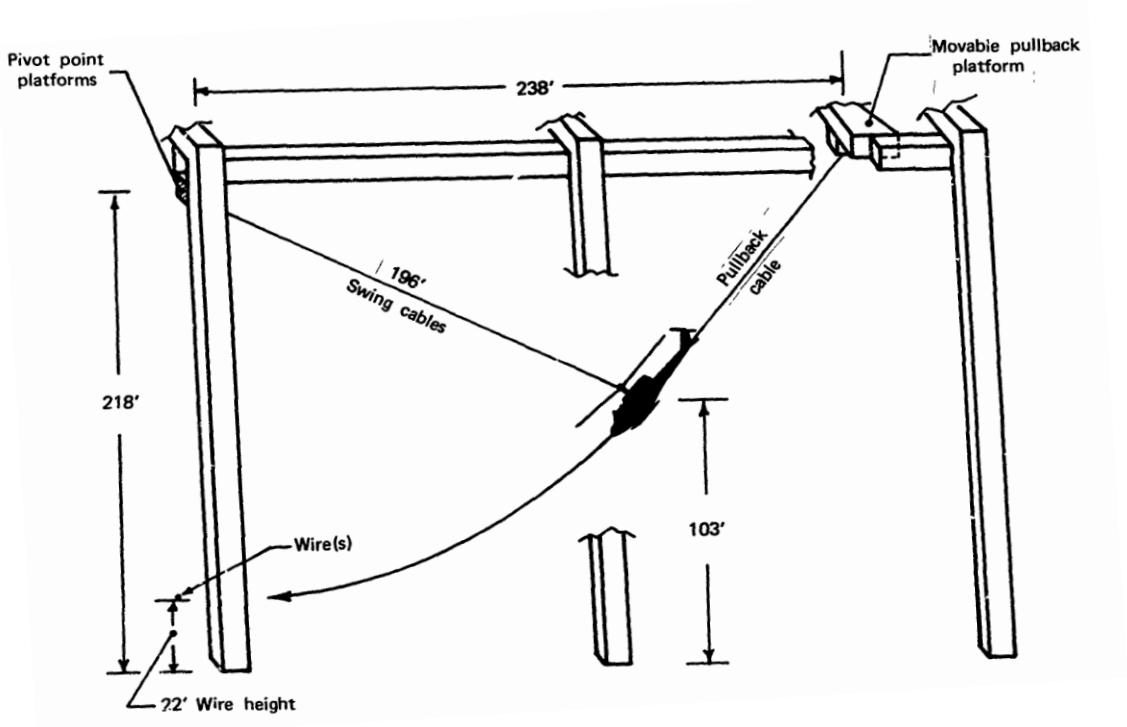

Figure 6.3: Swing Test Setup (Burrows L. T., 1982)

The helicopter was connected to a pivot point using a swing cable through its rotor mast. The rotor blades were detached from the fuselage for the purpose of testing. Additional weight was added to maintain the center of gravity (CG) near the rotor mast. The fuselage was pulled back to a desired height using a cable attached to the tail end. The pull-back height was determined based on the speed required during the impact. The cables were arranged in such a way that the helicopter would impact them at a pitch angle of almost zero. Most of the tests occurred at 40 knots impact speed. In order to get an accurate measurement of the aircraft attitude, gyroscopic sensors were installed on the fuselage to measure pitch, roll, and yaw attitudes. Accelerometers

were placed inside the fuselage to measure accelerations in all three directions. Loads during impact could be calculated from the accelerometer data. The tension in the cable was monitored using load cells, and an external radar system was used to calculate the helicopter speed during impact. The entire experiment was captured on high-speed cameras (650 frames/s) for further analysis.

The tests revealed that the change in pitch attitude due to impact is not significant for cables striking the windshield and reaching the upper cutter. This was expected as the center of gravity is located almost in the same horizontal plane as the upper cutter, leading to a low pitching moment. The aircraft pitch angle varies with time due to the pendulum-like motion. Figure 6.4 (a) reveals that the pitch angle deviation from its regular motion due to impact is not significant. It is interesting that pitch-angle variation for the lower-cutter impact, shown in Figure 6.4 (b), is very similar to the one for the upper cutter.

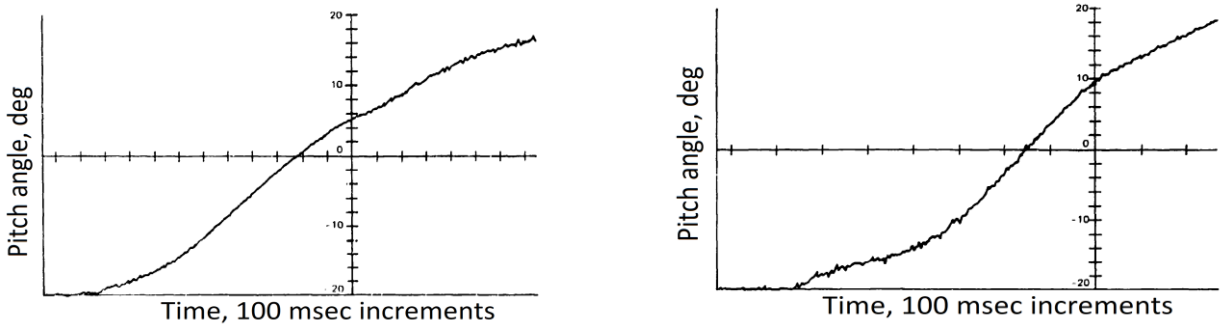

(a) Upper Cutter Impact

(b) Lower Cutter Impact

Figure 6.4: Pitch Angle Variation during Swing Test (Burrows L. T., 1980)

Even though the moment arm is larger for the lower cutter, significant changes in pitch attitude due to impact were not observed. As mentioned previously, forces acting on the fuselage may be determined from the acceleration data, as displayed in Figure 6.5 and Figure 6.6 for the longitudinal and lateral accelerations, respectively. According to Burrows (Burrows L. T., 1980), the stresses generated due to these forces are well within the critical range of fuselage handling capabilities. These forces are also considered not high enough to affect crew performance or the flight attitude.

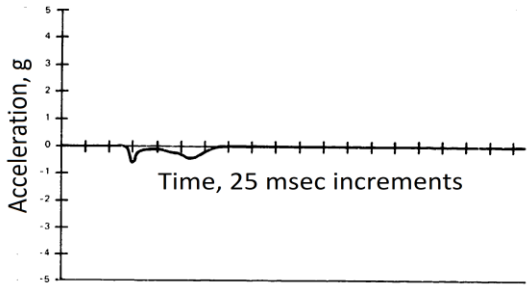

Figure 6.5: Longitudinal Acceleration Time History (Burrows L. T., 1980)

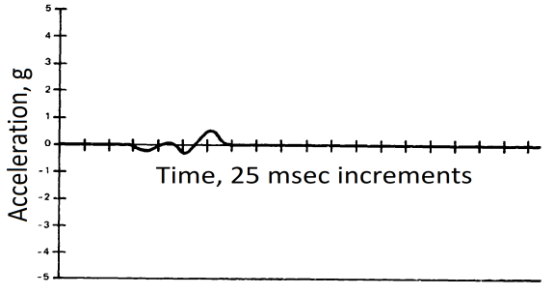

Figure 6.6: Lateral Acceleration Time History (Burrows L. T., 1980)

The windshield and deflector integrities were also examined as part of the tests. The deflector edge is made of serrated blades, to cause maximum damage to the wire before reaching the cutter. Tests showed that the deflector was able to cut thin wires upon impact, but for larger wires (such as a 10M cable), the serrated blades suffered damage and were not able to cut the wire on their own. Tests on the UH-1 helicopter showed that the deflector and windshield were able to withstand impact, but that the cable did not reach the cutter as it was caught in the windshield-wiper shaft. The wiper shaft failed on contact as the cable entered the cockpit, which could be dangerous for the crew. An additional deflector was designed for the windshield wiper to guide the cable away and into the cutter. Subsequent tests proved this design to be effective.

The cable-cutting process was captured on high-speed cameras and some of the images from the footage are shown in Figure 6.7.

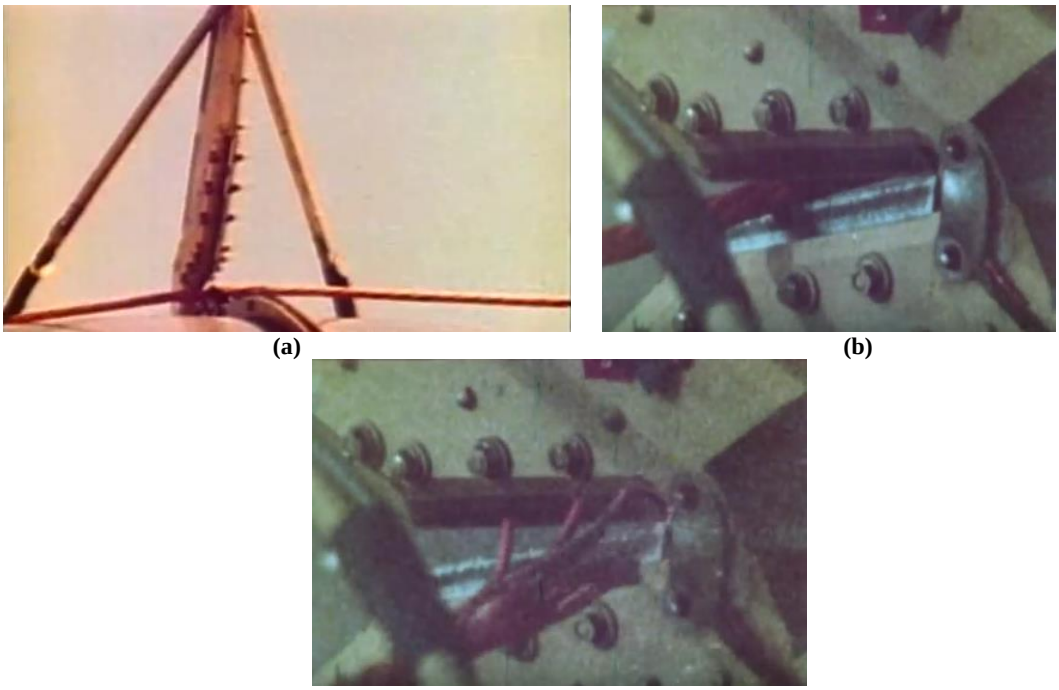

Figure 6.7: Wire Cutting Process by the WSPS[46]

Advantages of the WSPS

- Passive system
- Lightweight
- Easy maintenance

Disadvantages of Passive Wire Cutter System

- System may not be effective at low speeds
- If insufficient tension is created in the cable, failure might not occur
- Aircraft could decelerate drastically if the cable is not severed immediately upon impact
- Direction of aircraft could change

[46] *https://www.youtube.com/watch?v=rm6MwIdY4TA* [Last accessed on 01/31/2019]

- Aircraft could get entangled in surrounding cables
- Cutter effectiveness is based entirely on kinetic energy of aircraft
- Additional reinforcements are required to withstand loads transferred to the airframe

6.2 ACTIVE WIRE CUTTERS

Some of the disadvantages of passive wire cutters may be overcome by active cutters. Various concepts for active-wire-cutter systems are described in McKown's patent (McKown, 1989). A typical active-cutter system mentioned is shown in Figure 6.8. The system has a movable cutter with a V-notch. As a cable enters the cutting assembly, the V-notch swings back about a pivot point, following an arc trajectory. A piston in contact with the V-notch is pushed backwards and triggers a cartridge, placed at the other end of the piston, by bringing it in contact with a trigger pin. The explosion drives the piston forward rapidly, which, in turn, forces the V-notch to cut the cable by swinging forward.

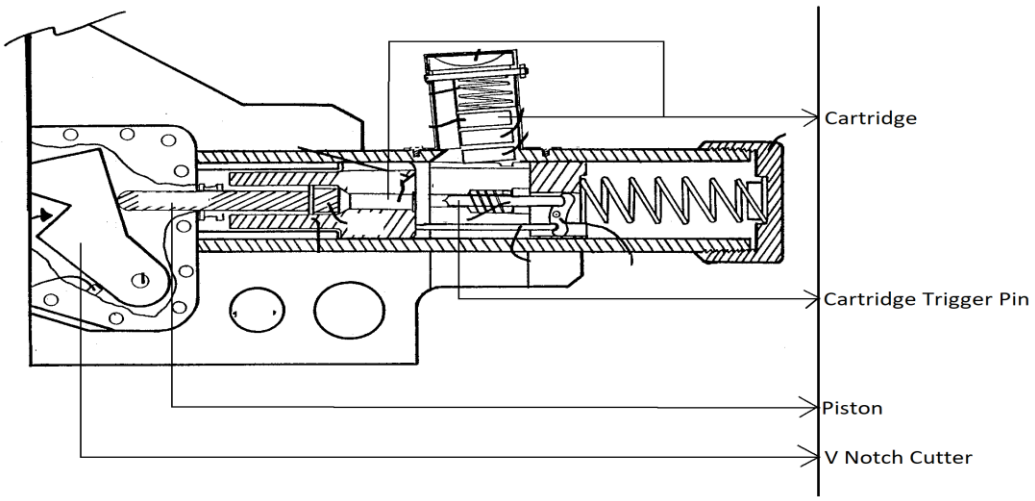

Figure 6.8: An Active Wire Cutter (McKown, 1989)

A cartridge magazine is placed behind the cartridge trigger, such that as the explosion occurs, the used cartridge falls out of the cylinder and is replaced with a new cartridge from the magazine placed above. The system is reset and ready for further firing if needed. This mechanism ensures that the cable is cut regardless of the speed of the vehicle, as long as the cable enters the cutter assembly and moves the cutter enough to trigger the system. Currently, no active wire-cutter system is available commercially or installed on helicopters.

Advantages of Active Wire Cutter System

- Effective even at low speeds
- Can operate in a wide range of aircraft orientations
- Even cables without tension can be severed
- Load transferred to airframe is minimal as wires are severed immediately upon impact

Disadvantages of Active Wire Cutter System

- More complicated than passive wire-cutter systems
- Number of cuts depend on number of cartridges

- Careful maintenance procedure required

Several other active wire-cutter patents exist describing various cutting mechanisms. Two such mechanisms are shown in Figure 6.9 and Figure 6.10. The cutter in Figure 6.9 has two wedge-like cutting surfaces that move against the wire surface. They act like a saw mechanism in the cutting process. The surfaces are moved by a cutter wheel that rotates about a pivoted point. Multiple cutter surfaces can be attached to the wheel to increase the efficiency of the cutting process. The wire cutter shown in Figure 6.9 has a probe fitted with multiple active wire cutters facing forward. Any wire encountered by the probe will be sent through multiple explosive cutters until it is severed. The cutters hold the cable until a detonation mechanism tries to sever the cable. If the cable is still intact, it will slide down to the next cutter along the probe. Due to the complexity of the mechanism and the mass and drag properties of the probe, this cutter could be impractical.

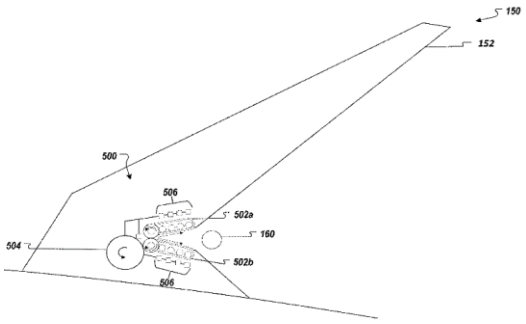

Figure 6.9: Active Wire Cutter (Smith, Tho, & Marimuthu, 2017)

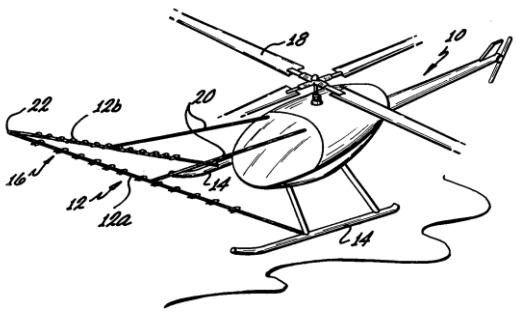

Figure 6.10: Wire Cutter Probe (Emigh & Goldin, 1983)

Less dependency on external factors make active wire cutters an ideal choice for lightweight helicopters. A new active wire cutter could be designed to overcome the disadvantages of the systems described in this section.

7. FRACTURE MECHANICS MODELING

In order to design a wire cutter for lightweight helicopters, it is essential to understand the wire-cutting mechanism and the forces involved. Estimating the force required to cut a cable under tension would enable the determination of the minimum helicopter speed required to cut a cable without adverse effects to aircraft handling or crew performance. This may be achieved in three different stages as shown in Figure 7.1.

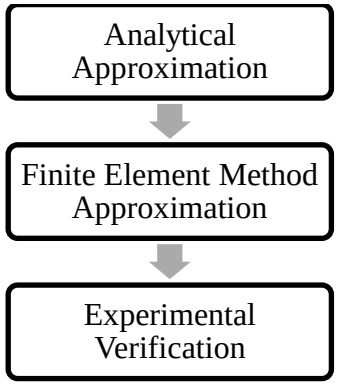

Figure 7.1: Stages of Load Estimation

The first stage is to formulate different aspects of the problem. The entire cutting mechanism may be divided into three main categories: dynamic loading due to impact, notch/crack nucleation by the cutter, and growth of the crack under multiaxial loading until failure. Creating a crack or notch at the surface of the cable is a vital step in the cable-severing process. Contact mechanics govern the forces and stresses at the point of contact between the cable and the knife edge. The magnitude of the forces vary, depending on the impact velocity. Dynamic loading cases will be discussed later; first, it is important to formulate a relationship between the external load and the stresses in the cable.

7.1 CONTACT MECHANICS

The contact problem was first addressed in 1881 by Hertz (Hertz, 1882). Hertz studied contact forces between two elastic spheres (general case), assuming that the surfaces are frictionless, the strains are within elastic limit, and the surfaces are continuous. Upon contact, the spheres deform, contacting each other over a circular region. Hertz derived an expression relating displacement, pressure, and resultant contact force. From these relationships, stresses inside the body were later derived by Huber (Huber, 1904). This became the foundation for contact problems.

Several other load scenarios are discussed in a book by Johnson (Johnson, 1985). For example, a normal “concentrated line load” acting on a semi-infinite body represents a knife-edge pressing into a plane surface. Polar coordinates are used to obtain the stress distribution in the near load region. Stresses far away from the point of load application turn out to be zero, as expected, but the stress at the point of load application is infinite. This is due to the “concentrated line load” assumption and does not represent actual behavior. This assumption makes it difficult to find the actual stress for knife edge and sphere contact. A normal concentrated load instead of a

concentrated line load is discussed by Johnson (Johnson, 1985). In this case, the problem is axisymmetric and the stress distribution is three dimensional, unlike in the previous example.

The contact of cylindrical bodies was also discussed by Johnson (Johnson, 1985). An elastic circular cylinder in contact with two surfaces at diametrically opposite ends was studied. The long cylinder was subjected to contact forces in the plane perpendicular to the axis of the cylinder. A Hertzian pressure was assumed to be acting on the point of contact along with concentrated forces and bi-axial tension. The stress distribution over a cylinder with concentrated loads is described by Timoshenko and Goodier (Timoshenko & Goodier, 1951). The stress scenario for all these cases were linearly combined to obtain the stress state for this case.

It is interesting to note that the WSPS system severs the wire by slicing and pushing into the wire due to its geometric orientation. Hence, it is not enough to study just the normal forces in contact. The problem of "cutting by slicing" with shear and normal forces is studied by Reyssat et al. (Reyssat, Tallinen, Merrer, & Mahadeva, 2012). The forces required to cut a very soft material using a thin wire were measured experimentally. It was observed that the normal force required to cut the material decreased significantly when a shear force was introduced. Finite element analysis was performed to compare the model with experimental results and a good correlation was obtained between the two approaches.

Another way of studying the cutting mechanism is by using a fracture-energy approach, in which the amount of work done during slicing and pushing is equal to the fracture work done to grow the crack (Atkins, 2009). Once the slide-push ratio is fixed, the force required to cut through a specimen of a given material may be obtained if the fracture toughness is specified; however, the specific case discussed in Atkins (Atkins, 2009) is for a rectangular block. The formulation must be derived for the case of a cutter entering in contact with a cylindrical wire. One important note is that the force required to initiate the cutting process is not discussed in the aforementioned study. For the initial infinitesimal area, the force required to cut turns out to be zero. However, this is not true. In fact, the force required to initiate the cut is large as shown by Reyssat et al. (Reyssat, Tallinen, Merrer, & Mahadeva, 2012). A soft material is cut by slicing, i.e. by applying both normal and shear forces. Before the cut is initiated, the normal force increases linearly with an increase in surface displacement, as depicted in Figure 7.2. As the cut is initiated, the normal force required to penetrate the material reduces rapidly for the same displacement.

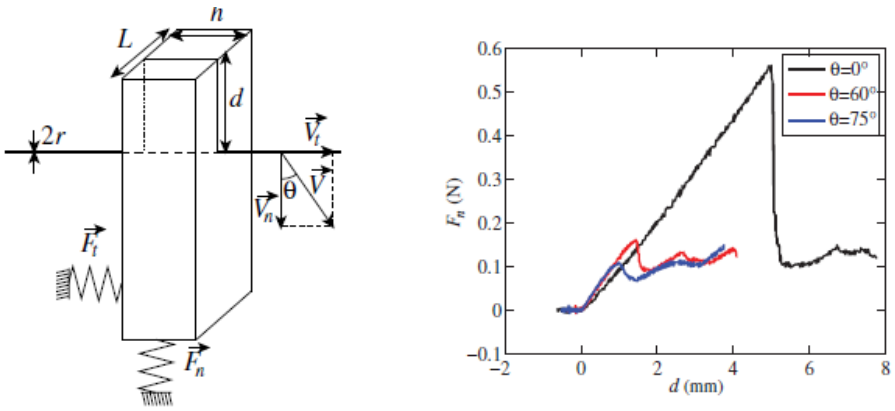

Figure 7.2: Force Required to Initiate a Crack in Soft Material (Reyssat, Tallinen, Merrer, & Mahadeva, 2012)

7.2 CRACK PROPAGATION

Once a notch/crack is created on the surface of the cable, its growth can be predicted based on the stress condition, the material property, and its geometry. Prediction of crack growth based on initial crack length and loading has been a crucial part of fatigue and fracture mechanics. Fatigue crack growth has been studied extensively using Paris's law and its variations. A few studies have been carried out to obtain analytical expressions for crack propagation under monotonic loading conditions. For example, McClintock (McClintock & Argon, 1966) provides a crack-growth criterion based on a plastic-strain assumption for a crack under Mode III loading condition (out-of-plane shear). Griffith and Taylor (Griffith & Taylor, 1921), studied crack growth in glass, a brittle material, and developed a crack-growth criterion based on energy. According to Griffith, crack propagation occurs when the elastic energy released due to crack growth is greater than or equal to the energy required to create a traction-free surface. In his book, Anderson (Anderson, 2005) discusses a criterion for crack extension based on energy release rate and resistance of material to crack extension. The downside of this approach is that the resistance of the material to crack extension must be obtained through experimental analysis if the data is not available. Irwin (Irwin, 1962) further provides an analytical relationship between crack length, far-field stresses, and stress intensity factor, considering plasticity in ductile materials for a plate with a semi-elliptical crack. However, this study deals with a static crack. Due to the complex mechanisms involved in crack propagation, most of the studies on crack propagation are either experimental or numerical.

Fatigue-crack growth in cables has been studied mostly in the context of bridge construction. For example, Mahmoud (Mahmoud, 2007) studied the fracture strength of bridge steel-cable wires subjected to both tensile and flexural loads. These multiaxial stress effects were included to study crack growth in steel wires with surface cracks. The crack front in cylindrical structures can be semi-circular or straight. A straight crack is found to have a higher stress intensity factor compared to a semi-circular crack of the same length. Higher stress-intensity factors lead to higher crack-growth rates according to Paris's equation in the Linear Elastic Fracture Mechanics (LEFM) regime. The stress intensity factor for both of these cases was found using the Finite Element Method (FEM) analysis and also from literature data (Caspers & Mattheck, 1987). Caspers and Mattheck (Caspers & Mattheck, 1987) consider crack fronts for bars under several

loading conditions, and compute stress intensity factors using a weighted function method. The values obtained from the analytical method were compared with 3-D FEM values and found to be in good agreement. Once the relationship between stress intensity factor and crack length is established, the critical length of the crack that leads to failure may be estimated.

The study performed by Mahmoud (Mahmoud, 2007) was extended by Sih et al. (Sih, Tang, Li, Li, & K.K.Tang, 2008) to cables with multiple strands. The cables of the Runyang bridge were studied, under varying tension loads, using a two-scale model. Both a micro-crack growth model and a macro-crack growth model were used to account for different behaviors of crack growth within a wire and a cable (Sih, Tang, Li, Li, & K.K.Tang, 2008). Material properties were chosen carefully to capture this difference in behaviors. Cables with varying cross-sectional areas, allowing for gaps between wire strands, were subjected to cyclic tensile loads and the increase in crack length was computed using semi-analytical equations. The results obtained for cables were compared with crack growth in wires to determine whether the critical values of crack length agreed. Higher tensile stresses led to higher crack growth rates and the smaller the gap between the strands, the better the fatigue performance of the cable.

7.3 IMPACT LOADING

For any case involving impact loading, inertial effects must be taken into consideration. Inertial effects increase the loading in a dynamic load situation compared to a static load case; however, considering the transient behavior of a system during dynamic loading can be very complicated and time consuming. To avoid this, an Equivalent Static Load (ESL) is considered for studying dynamic systems. The idea is to amplify the static loads by an "impact factor" to match the dynamic displacements or stresses. The impact factor can be obtained from energy methods as described by Akin (Prof. J. E. Akin) and by Thompson (Prof. B. S. Thompson, 2005). Several textbooks also describe impact factors for various scenarios. For example, Choi and Park (Choi & Park, 1999) transform dynamic loads into ESLs using modal analysis. An approximate analytical expression was obtained between ESLs and dynamic loads by imposing a condition that the displacement fields must be similar. Similarity between these fields is ensured at critical times, specifically when the displacement is at extrema. Hence, for a given dynamic load, equivalent static loads can be obtained with some approximations. Choi and Park created finite-element models of beams and trusses for dynamic loads, and solved for displacements as a function of time (Choi & Park, 1999). The ESLs were obtained based on the proposed modal analysis technique. The ESLs obtained were used to solve static beam and truss problems in ANSYS and compared with the dynamic displacement field. The results agreed with each other to a fair degree of accuracy.

An equivalent static load for dynamic impacts in automobile chassis was studied by Dattakumar and Ganeshan (Dattakumar & Ganeshan, 2017). The ESLs were obtained using Global Response Surface Method (GRSM), a system-identification technique. In this technique, the global input variables are varied until the required output is obtained. The authors used Hypermesh[47] for meshing their domain and carried out dynamic simulations using RADIOSS[48], an FEM solver. Various types of impulse loads (trapezoidal, triangular, and sinusoidal) were considered in this

[47] https://altairhyperworks.com/product/HyperMesh [Last accessed on 01/31/2019]
[48] https://altairhyperworks.com/product/RADIOSS [Last accessed on 01/31/2019]

study. Equivalent static loads for this dynamic field were obtained by carrying out an optimization procedure in Hyperstudy[49]. The response of the system was very sensitive to the duration and shape of the impulse loads.

A more realistic way of treating dynamic impact loads is to consider wave propagation inside the structural elements. When a structure is subjected to impact at the surface, stress waves propagate inside the structure. These stress waves can be compressive or tensile depending on the load applied and on reflections occurring within the boundaries of the system. Governing equations of wave propagation in an elastic medium and a few examples of wave propagation due to impact are discussed by Timoshenko and Goodier (Timoshenko & Goodier, 1951).

Moon et al. (Moon, et al., 2006), studied the impact of thin glass plates used in LCD display screens. They suggested a new technique to obtain equivalent static loads for a dynamic system to reduce the design-cycle time of LCD screens. A finite-element beam model, representing a thin screen and considering shock propagation, was created in LS-DYNA[50], The modelled thin screens were subjected to impact loading. The displacement and stress fields obtained from Finite Element (FE) analysis were compared with analytical solutions. After validating the FE model, the ESL was obtained by equating the strain energy of the static problem to the internal energy of the impact problem. A relationship between the maximum stresses of both cases was also obtained.

The ultimate goal of these analyses was to obtain a relationship between the ESL and the dynamic loads. This can be carried out either by including the wave propagation, or by considering only the impact factor, or both. Including shock waves makes the analysis more complicated. Shock waves travelling across a cylindrical cross section, like a cable, imply mathematical complexity. Hence, in the case of a wire strike by a lightweight helicopter, we may ignore shock waves to obtain the ESL. In case this is insufficient, further analysis will be carried out. The overall goal of the analytical analysis and the fields of study involved are shown in Figure 7.3.

[49] https://altairhyperworks.com/product/hyperstudy [Last accessed on 01/31/2019]
[50] http://www.lstc.com/products/ls-dyna [Last accessed on 01/31/2019]

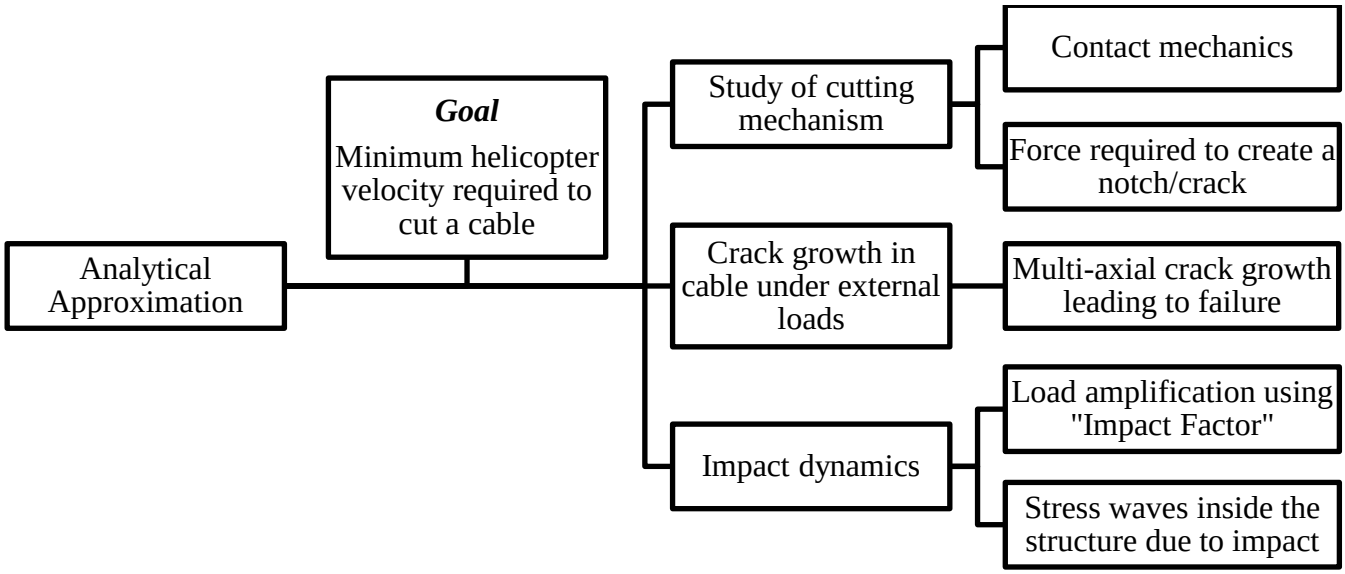

Figure 7.3: Tasks Associated with Analytical Approximation

7.4 GAP IN THE LITERATURE

Our literature review revealed that significant, but independent, research has been carried out in all the different aspects of problem of protecting against helicopter wire strikes. . Research combining all these fields to tackle a single problem is almost non-existent in the public domain, as depicted in Figure 7.4. We believe that it is important to bring these different areas of structural mechanics under the same umbrella in order to tackle successfully the issue of helicopter wire-strikes. These scenarios are unique to our problem and have not been addressed elsewhere. Hence, it is highly recommended to push future research in this direction.

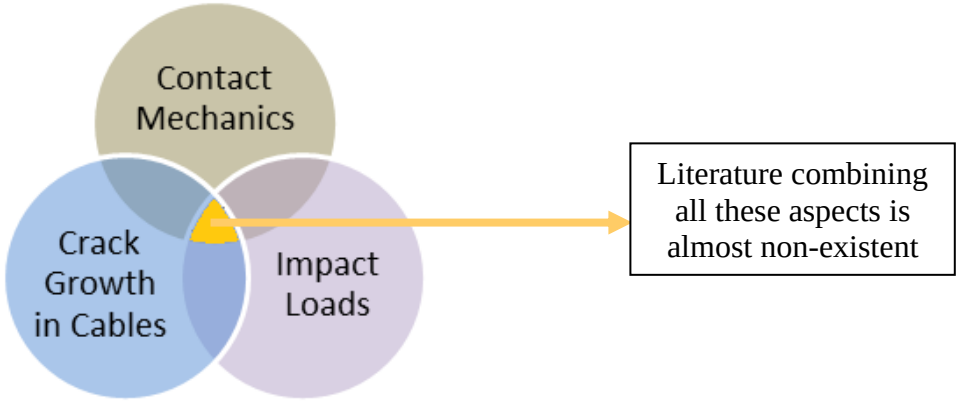

Figure 7.4: Missing Research Domain in the Literature

7.5 FINITE ELEMENT METHOD (FEM)

Finite-element methods are used extensively in the analysis of deformable structures because FEMs provide approximate numerical solutions to problems which are difficult or impossible to solve analytically. FEM has been used widely in the study of impact dynamics to determine ESL,

as discussed in section 7.3. For example, Müllerschön et al. (Müllerschön, Erhart, Anakiev, Schumacher, & Kassegger, 2013) describe the analysis of impact problems using LS-DYNA, a commercial FEM software. The non-linear displacement field of thin plate-like structures during a crash into a rigid wall was obtained from impact analysis in LS-DYNA to evaluate the ESL. Using the ESL obtained, an optimization of the profile was carried out using the GENESIS[51] software. The analysis was extended to the optimization of the geometry of the inner hood of a car to increase safety during crashes.

A lecture by Dassault Systems (Dassault Systems) describes almost every technique available in Abaqus[52] for modeling and analyzing cracks. For modeling sharp 2-D cracks, nodes on the opposite edges of the crack are disconnected but there is no visible gap between them in unloaded conditions. Sharp 2-D cracks are called "seam cracks." The crack tip is modelled with concentric triangular elements. Cracks in 3-D are modeled using C3D-series elements. The crack-trip mesh density is maintained to be larger than the surrounding regions, to capture the high-stress gradient. Notches, which are cracks with significant thickness and a blunt tip, can be modeled similarly to sharp cracks. The damage of structures due to impact can also be modeled by defining the contact behavior. The definition of the contact behavior also allows the study of impact loadings. Failure of structures can be studied dynamically by the Damage Evolution module of Abaqus. One useful feature of Abaqus to study the cutting mechanism is the element removal option: Mesh elements get removed automatically as they reach critical stress/strain values, simulating the formation of notches or cracks.

The crack front whose path of propagation is undetermined can be studied using XFEM[53] (eXtended Finite Element Method). This feature allows the crack to grow, even through the mesh boundaries, making it desirable for practical applications. The damage-initiation criterion can be specified either in the form of stress or in the form of strain. Crack initiation and crack propagation can be studied using XFEM elements.

The tasks that should be performed when designing a wire cutter for lightweight helicopters are summarized in Figure 7.5. The goal is to build FEM models of a cutter and a cable with appropriate finite elements to handle contact and impact loads. Simulation of a wire strike event may then be carried out and results may be compared with results obtained from the analytical approximation discussed in the previous sections.

[51] https://www.esha.com/products/genesis-rd/ [Last accessed on 01/31/2019]
[52] https://www.3ds.com/products-services/simulia/products/abaqus/abaquscae/ [Last accessed on 01/31/2019]
[53] http://www.xfem.rwth-aachen.de/Background/Introduction/XFEM_Introduction.php [Last accessed on 01/31/2019]

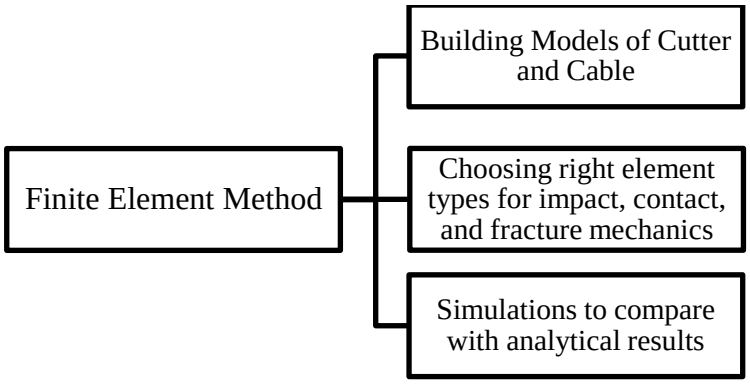

Figure 7.5: Objectives of the FEM Analysis

8. CHALLENGES AND OBSTACLES TO THE IMPLEMENTATION OF WIRE CUTTERS ON LIGHTWEIGHT ROTORCRAFT

Wire cutters are widely used on medium and heavy-weight helicopters, but they are not popular or available for lightweight helicopters. Helicopters with a maximum take-off weight (MTOW) below 7,000 lbs (3175.14 kg) are considered lightweight by the FAA and the EASA[54]. EASA provides an additional category, called very light rotorcraft, for helicopters with MTOW below 1,320 lbs (598.74 kg). Some of the challenges that could be faced while designing and installing wire cutters on lightweight/very lightweight helicopters are as follows:

1. The surface area available for installation is limited due to the small airframe size. Lightweight helicopters are also designed with large windshields to provide better situational awareness to the pilots. This further reduces the metal surface area available to affix the wire cutter. Figure 8.1 shows a lightweight helicopter with large windshields.

Figure 8.1: Robinson R22 Helicopter[55]

2. Attaching a wire cutter to a glass surface may not be effective. Glass is a brittle material, and brittle materials do not perform well on impact due to their relatively low ability to absorb fracture energy. Brittle materials also have relatively low tensile strength, which further makes them undesirable to handle tension stresses arising from bending moments during wire strikes. Installation on glass will also be difficult as creating new holes might lead to crack nucleation.

3. Per item 2 above, the wire cutter system would need to be installed very close to the rotor mast, where a metal surface is available. This, in turn, would leave most of the rotor unprotected from wire strikes.

4. The mass of the helicopter affects the efficiency of wire cutters. The lower the mass of the helicopter, the greater the deceleration required to produce the same amount of force needed for a successful cut. Such quantities will need to be computed quantitatively and qualitatively.

---

[54] *https://www.aeronewstv.com/en/lifestyle/how-it-works/3277-civilian-helicopters-heavy-or-light.html* [Last accessed on 01/31/2019]

[55] *https://robinsonheli.com/r22-specifications/* [Last accessed on 01/31/2019]

5. Increasing the tension in the cable is essential for crack growth after a partial cut is made by the wire cutter. Due to the lower inertia of lightweight helicopters, could allow it to decelerate drastically while removing slack from the cables in order to increase the tension.

6. Wire-cutter installation could be challenging due to other essential equipment that needs to be installed on the airframe. An example is shown in Figure 8.2, where a camera obstructs the lower cutter. This could prevent any wire from reaching the cutter, resulting in additional pitching moments during a strike. Overlap of equipment space will be more prominent for lightweight helicopters due to their limited installation-surface area.

Figure 8.2: Camera Obstructing Lower Wire Cutter on the Bell 429[56]

The only helicopter that is close to the very lightweight category and that has an installed WSPS system is the Robinson R66. The R66 has a maximum gross weight of 2,700 lbs (1224.69 kg). The wire-cutter system for the R66 was certified by the FAA and installed on an R66 helicopter at the beginning of 2018. The WSPS for the R66, priced at $22,800, weighs 16 lbs including all the installation equipment. A depiction of the WSPS system on an R66 is shown in Figure 8.3.

Figure 8.3: WSPS on R66[57]

[56] https://www.helis.com/database/news/apscon18-bell-429-nassau/ [Last accessed on 01/31/2019]
[57] https://robinsonheli.com/press-releases/wire-strike-protection-r66-helicopters/ [Last accessed on 01/31/2019]

9. WIRE STRIKE SAFETY TECHNOLOGIES CLASSIFICATION

All the wire-strike safety technologies discussed in this report can be categorized as shown in Figure 9.1. It is interesting to note that there are no readily available active wire-strike protection systems. Also, there are no readily available passive aircraft-mounted prevention systems or passive ground-based protection systems. In order to develop new safety technologies, one could focus on these missing technologies.

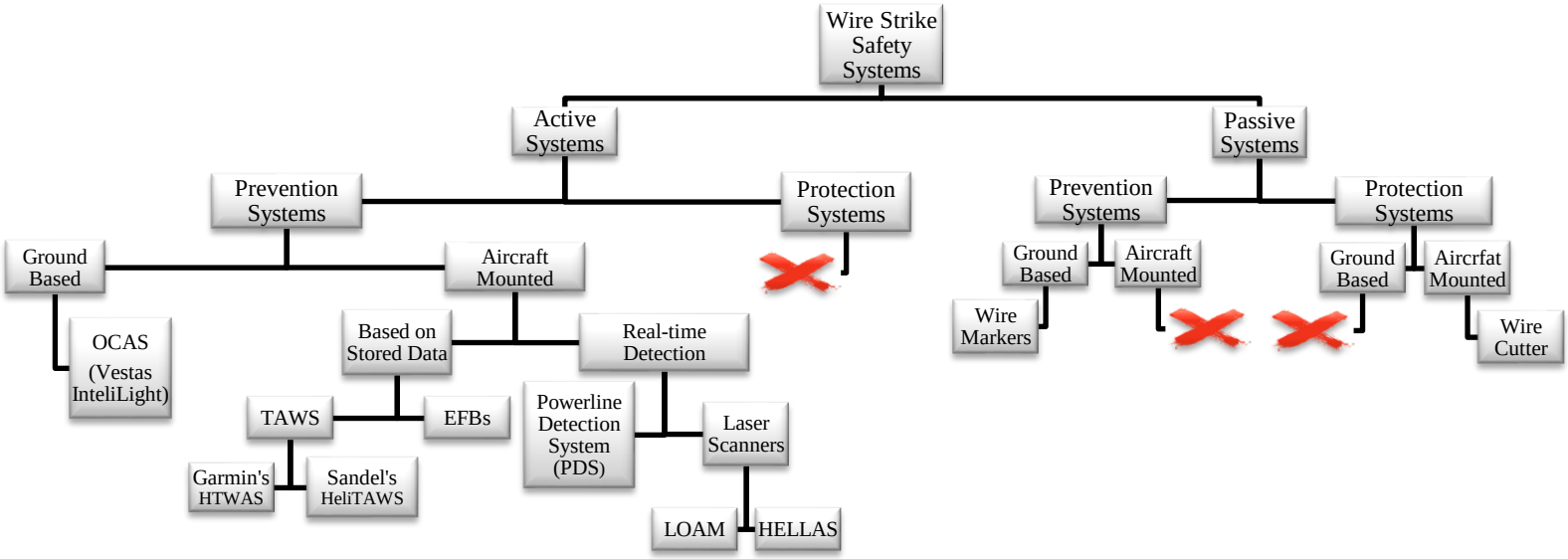

Figure 9.1: Summary of Wire Strike Safety Technologies

10. OTHER POTENTIAL HELICOPTER SAFETY TECHNOLOGIES

This section discusses a few technologies used in other fields of aviation or other industries that have the potential to be applied to helicopter safety, either directly or after some modifications.

10.1 UNMANNED AERIAL VEHICLE TECHNOLOGIES

Unmanned Aerial Vehicles (UAVs) have become increasingly popular following the advent of brushless motors and wireless technologies. They are used for a wide variety of applications from military to research to recreational activities. UAVs fitted with high-resolution cameras are commonly used for photography and video blogging. As a result of their advanced control capabilities, they are becoming more and more autonomous. As their level of autonomy increases, it is essential to prevent UAVs from colliding with obstacles. This has led to the use of multiple sensors and processing algorithms to handle multiple data inputs. A typical commercial UAV is shown in Figure 10.1, along with some of the sensors commonly used.

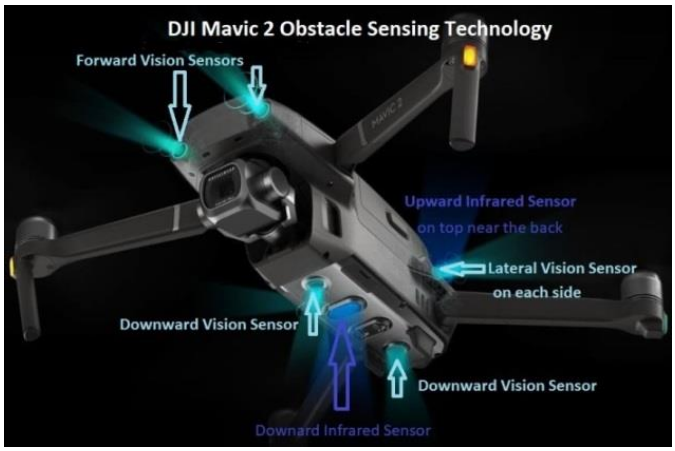

Figure 10.1: DJI Mavic 2 Pro/Zoom Obstacle Sensing Drone[58]

Some of the obstacle-avoidance sensors used on these UAVs are discussed in the subsequent sections.

10.1.1 Stereovision

A stereovision system uses two cameras placed side by side to determine the depth of objects in the field of view. The images formed inside the two cameras are offset from each other depending on the location of the object, as shown in Figure 10.2. A computer algorithm compares these two images and tries to find the matching pixels. Once the pixels are matched, the distance to the object is determined by geometrical relationships.

The stereovision system can predict the depth field of an entire image. The DJI Mavic 2, shown in Figure 10.1, has stereovision systems fixed to the front, side, and bottom. Depth information obtained in real time is used by the UAV control system to avoid obstacles. The image to the left

[58] *https://www.dronezon.com/learn-about-drones-quadcopters/top-drones-with-obstacle-detection-collision-avoidance-sensors-explained/* [Last accessed on 01/31/2019]

of Figure 10.3 shows the depth information of the image to the right. Objects closer to the camera are colored in red and objects farther away are shown in blue.

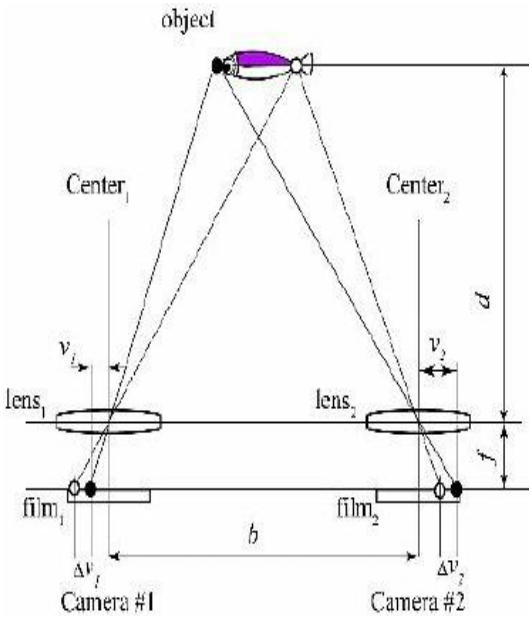

Figure 10.2: Stereovision Principle (Yoshida, 2009)

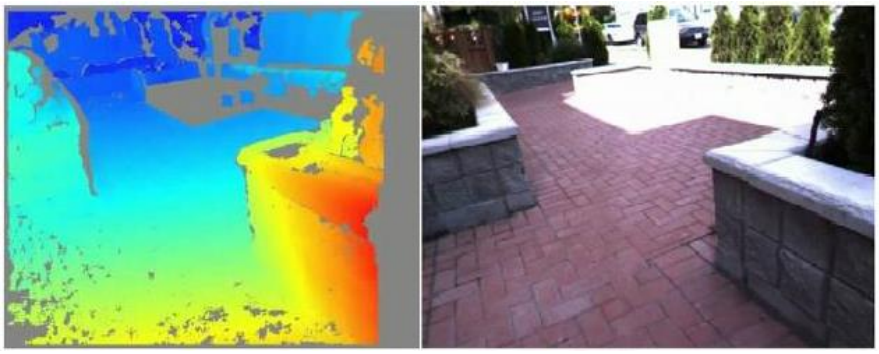

Figure 10.3: Stereo Vision[59]

A similar configuration of stereovision can be used for helicopters to detect obstacles in real time. With increased resolution and range of stereovision, wires of various diameters could potentially be detected and avoided.

10.1.2 Ultrasonic Sensors

Ultrasonic sensors are used on the DJI Mavic Pro, along with a stereovision system, to obtain altitude information that the UAV uses to maintain a constant height from the ground as it flies. Sensors send ultrasonic waves toward the ground and listens to the bounced-off waves. Distance information is calculated from the time taken for a wave to travel from a sensor to the ground

[59] https://www.youtube.com/watch?v=Ckd1KJZreVE [Last accessed on 01/31/2019]

and back. This sensor, shown in Figure 10.4, is a miniature version of the sonar technology used in ships and submarines.

Figure 10.4: Ultrasonic Sensor[60]

Due to their small size, the range of these sensors is limited to 4 meters, but external noise and gusts can further lower this range. Tilted and soft surfaces (e.g. water, plants) can affect the quality of the reflected signal. Notwithstanding these problems, an enlarged version of this sensor could be used onboard helicopters to detect obstacles, including wires. Since a helicopter tends to generate a lot of noise and airflow around the airframe, the operating frequency of the sonic sensor would need to be chosen carefully to successfully detect obstacles in the vicinity.

10.1.3 Time-of-Flight Sensor

A Time-of-Flight (ToF) sensor is very similar to an ultrasonic sensor, but it uses light waves instead of sound waves. A typical ToF camera for UAVs is shown in Figure 10.5. A ToF sensor has a lens with its own light source, which it uses to illuminate a scene in either short bursts of visible light or continuous infrared. When using short bursts of light, the time it takes a pulse of light to travel from the source and back to the sensor is measured to determine the distance of each pixel. During continuous illumination, the phase-shift of the light is used to get the distance information. Hence, the ToF sensor determines the depth of the entire scene from a single captured image, as shown in Figure 10.6. This makes it the fastest sensor to capture depth information. Due to high refresh rates, it is advantageous to use ToF sensors for high-speed applications in which the scene changes rapidly, as in helicopter flights.

The ToF sensor does have some disadvantages. First, it uses its own light source, hence making it almost impossible to use in daylight conditions (it very well suited for night operations). Second, multiple reflections from oddly shaped surfaces can lead to erroneous data. Third, the range of the ToF sensor is based on the strength of the light source. Nevertheless, with certain modifications and improvements to the existing technology, a ToF sensor for helicopters could be a strong contender for real-time obstacle detection.

[60] *https://www.theengineeringprojects.com/product/ultrasonic-sensor-hc-sr04* [Last accessed on 01/31/2019]

Figure 10.5: ToF[61]

Figure 10.6: ToF Image[61]

10.1.4 Solid-State LIDAR

A solid-state LiDAR system is similar to laser-scanner systems discussed earlier, but without any moving parts. A typical solid state LIDAR system has a fixed laser source and a sensor, as shown in Figure 10.7. The sensor divides the field of view into independent segments and detects the obstacles inside those segments within its range. The Vu8 system, manufactured by Leddar Tech, divides the field of view into 8 independent segments, as shown in Figure 10.8. The Vu8 can detect obstacles up to a range of 200 m and weighs only 75 g.

Figure 10.7: Vu8 Solid State LIDAR[62]

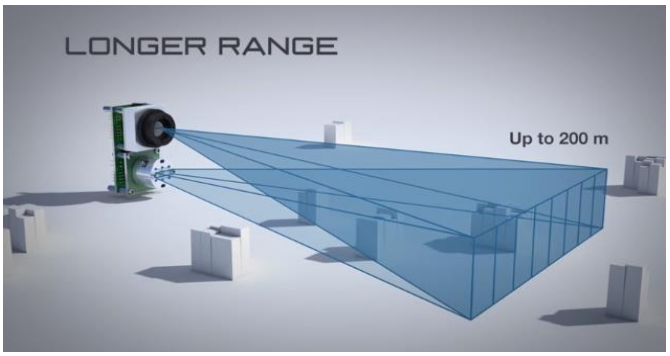

Figure 10.8: Vu8's Eight Independent Segments[62]

The sensor field of view and range could be varied depending on the requirements. The wider the view, the shorter the range. The absence of moving scanners makes the Vu8 quicker than other scanning systems. Leddar Tech claims that the Vu8 can work in direct-sunlight conditions and in adverse weather, such as rain and snow, thus providing an advantage over the ToF cameras discussed previously.

The resolution of the next-generation Vu8 system could be as fine as 0.25^{o} both in the horizontal and vertical directions. A solid-state LIDAR costs around $500, making it slightly costlier than wire-marker systems. Using multiple-sensor systems would provide 360^{o} coverage. Due to their high-speed detection, wide range of performance capabilities, light weight, and low cost, solid-state LIDARs should be considered for real-time obstacle detection on helicopters.

---

[61] *https://www.dronezon.com/learn-about-drones-quadcopters/best-uses-for-time-of-flight-tof-camera-depth-sensor-technology-in-drones-or-ground-based/* [Last accessed on 01/31/2019]

[62] *https://www.youtube.com/watch?v=-9Gbg5mjwm4* [Last accessed on 01/31/2019]

10.1.5 Data Fusion

Commercial unmanned aerial vehicles use multiple sensors to accurately predict obstacle locations. Data from different sensors are combined using a process called “data fusion”. The idea of data-fusion is that information from multiple sensors could provide greater accuracy and consistency than any single sensor. Similarly, multiple sensors and data-fusion techniques can be used on helicopters to detect wires and other obstacles.

11. SUMMARY, CONCLUSIONS, AND RECOMMENDATIONS

11.1 SUMMARY

Wire strikes were responsible for five percent of all helicopter accidents from 1963 to 2008. One third of these accidents were fatal and occurred in VFR conditions. Lightweight helicopters, like the Robinson R22 and the Bell 47, were involved in 35.5% of these wire-strike accidents. Hence, it is essential to equip these helicopters with devices that can warn and protect them and the crew from potential wire strikes.

11.1.1 Power lines and Cables Database

Transmission power lines have a major involvement in helicopter wire strikes. Databases containing the locations of all the power lines across the U.S. would help provide situational awareness and warn pilots of an impending strike. The North American power grid consists of four major divisions: Eastern Interconnection, Western Interconnection, Electricity Reliability Council of Texas Interconnection, and Quebec Interconnection. Combined, they consist of 580,000 km of transmission lines. The Energy Information Administration (EIA) provides an interactive map of power lines in the U.S. Using the FAA digital obstacle database, catenary information around Birmingham, Alabama, was plotted on Google Earth to demonstrate the potential of creating maps from tabular data. Development Seed (Development Seed, 2018) showed that a machine-learning algorithm could be trained to identify high-voltage towers from satellite images and create maps of power grids. This automated process was seventeen times faster than when the process was done by a human.

Power line cables come in various sizes and construction materials, depending on their purpose and voltage requirements. The American Wire Group provides a comprehensive database of static wires, guy wires, telephone wires, and electrical-transmission cables. Electrical-transmission cables are divided into several categories depending on their construction. The Aluminum Conductor Steel Reinforced (ACSR) power cables have a steel core surrounded by aluminum strands: the steel core provides mechanical strength and the aluminum outer layers provide a path for the current flow. In the All Aluminum Alloy Conductor (AAAC), the steel core is replaced by aluminum alloy cables and all strands are made of 6201-T81 aluminum. The Trapezoidal Aluminum Alloy Conductor Steel Reinforced (ACSR/TW) has a trapezoidal outer layer to make the cable more compact. Across all types, the strongest cable has a tensile breaking load of 142,800 pounds, and the largest cable has a diameter of 1.88 inches. The ALUM-18, which has a tensile strength of about 10,000 pounds, was the cable most commonly involved in wire strikes.

11.1.2 Wire Strike Prevention and Protection Systems

The majority of wire-strike accidents potentially could have been prevented if one or more safety devices would have been installed onboard, to warn of wires in the proximity or impending strikes. A Power line Detection System (PDS) can detect the electromagnetic field generated by active power lines and providing audio and visual warnings to pilots. The TAWS system displays contour maps of surrounding terrain and obstacles, based on onboard databases. A power-grid database has been incorporated into the TAWS by Garmin and Sandel to provide

warnings to pilots based on the trajectory of the flight. The WSPS is the only commercially available system to protect against an inevitable strike. The WSPS has two wire cutters fitted at the top and bottom of the front portion of the helicopter fuselage. The WSPS partially cuts the wire so that the cable fails under tension loads. Obstacle avoidance and warning systems can detect wires in real-time. These systems can scan the region in their field of view using eye-safe lasers and generate a map of the surroundings. An advantage of this system is that no database is required for its operation. Wire markers are the simplest way to make power lines more visible to aircraft flying at low altitudes. The FAA recommends an alternating pattern of orange, yellow, and white to make them more visible on different backgrounds. Wire markers are made of FRPs with UV-resistant pigment. The OCAS system is a ground-based radar unit, which warns aircraft on a collision course with the obstacle. The OCAS is a system mounted on an obstacle on the ground and warns pilots flying in the proximity when their aircraft is on a collision course with the obstacle. It is designed to operate in remote locations with low visibility and with minimal power requirements. Wire markers and OCAS are advantageous to helicopter operators as they do not need to be installed on the aircraft.

11.1.3 Electronic Flight Bags

Electronic Flight Bags (EFBs) are a digital version of traditional flight bags. The FAA defines an EFB as an electronic display system intended primarily for cockpit/flight deck or cabin use. EFBs reduce onboard weight and pilots workload. FliteDeck Pro by Jeppesen includes enroute charts, terminal charts, and Airport Moving Maps. FliteDeck can run on both Windows and iOS touchscreen devices. The VFR theme in FliteDeck Pro can display obstacles like power lines, suspended bridges, windmills, buildings, and towers. Jeppesen claims to have created the most comprehensive database of obstacles related to aviation. The NavAero t.BagC2^2 is a modular EFB designed to be integrated into the aircraft avionics system. The t.BagC2^2 has a portable CPU that runs on robust Windows XP. The t.BagC2^2 can be connected to satellite communication devices, video surveillance systems, aircraft data systems, and ground communication systems. Its modular design makes it easier to upgrade every part separately. The Aera 660 is a portable EFB by Garmin that can display a 3D terrain map of aircraft surroundings. The Aera 660 is equipped with GPS as well as GLONASS. Garmin has incorporated WireAware, a power line database, into the Aera 660 for display along with terrain information. The ForeFlight Mobile contains a comprehensive aeronautical map of most of the world. The information displayed on the map varies depending on the level of zoom. The software includes weather information such as turbulence data and icing information. The hazard avoidance feature of ForeFlight uses Jeppesen's obstacle database. The FlyQ is designed to minimize the time spent on the EFB while flying. The FlyQ includes 2D, 3D, and Augmented Reality (AR) aeronautical maps that run on iOS. In AR mode, Pilots can point their iPad camera in outside of the aircraft to visualize the closest airports on the screen. The HeliEFB is specially designed for helicopter operations. It is designed to focus on flight-management tasks like weight and balance, flight risk assessment, and emergency checklists. The Ramco EFB has the extended capability of handling maintenance and billing along with other flight-management tasks. Ramco tablets come with a stylus for easy use during flight.

11.1.4 Wire Strike Protection System

The Wire Strike Protection System (WSPS) is a passive wire cutter originally designed for KIOWA helicopters by Bristol Aerospace Limited (BAL). The WSPS was designed to cut cables under tension and is composed of cutters with two sharp, wedge-like mechanisms about 45^{o} apart. BAL conducted tests on the upper cutter installed on KIOWA helicopters by running it into cables at 15 to 60 mph. The tests were successful in severing the cable without damaging the fuselage (Burrows L. T., 1982). More detailed tests of the WSPS were performed by the U.S. Army during its certification process for the UH-1 helicopters. Full-scale swing tests on the KIOWA and the UH-1 were conducted at the Impact Dynamics Facility at NASA Langley. Change of pitch and yaw attitudes, deceleration loads, aircraft-handling properties, and windshield performance were studied in these tests. According to Nagaraj and Chopra (Nagaraj & Chopra, 2008), the WSPS is effective for helicopter speeds greater than 30 knots and impact angles greater than 60 degrees. In order to overcome these limitations, various active wire-cutter system designs were explored in several patents. Currently, active wire cutters are not commercially available.

11.1.5 Fracture Mechanics Modeling

Studying the cable-cutting mechanism is essential for designing an effective wire cutter. The cutting mechanism can be broadly divided into three categories: notch/crack nucleation by the cutter, growth of crack under multiaxial loading until failure, and dynamic loading due to impact. The crack nucleation at the surface of a cable is a critical step in the cutting process. The contact forces between the cable and the knife edge of the cutter need to be analyzed using contact mechanics. The WSPS system severs the wire by slicing and pushing into the wire due to its geometric orientation. The cutting mechanism can also be studied using a fracture energy approach. Once the cable is partially cut, the crack growth under tension loads needs to be studied. Since a helicopter wire strike involves a high-speed impact, inertial effects need to be taken into account. The equivalent static loads for the dynamic scenario need to be computed to analyze the contact between the cable and the cutter, and a FEM analysis of the cable-cutting mechanism may be carried out using commercial finite-element packages. The results of the analytical analyses may then be compared with FEM results.

11.1.6 Challenges to Implement Wire Cutters on Lightweight Helicopters

Magellan's WSPS is available for heavyweight and intermediate-weight helicopters. The system is not available for lightweight helicopters. This could be due to the limited metal surface area available for installation, the infeasibility of fixing the cutter on a glass surface, the low inertial forces during impact as a result of the low mass of the helicopter, and the deceleration of the helicopter being beyond the acceptable range during impact. These concerns related to the installation of a WSPS on a lightweight helicopter may be addressed effectively only after analyzing the problem quantitatively.

11.1.7 Other Potential Safety Technologies

Safety technologies used in other industries may be adapted to helicopter operations. For example, various types of sensors are used on UAVs to detect and avoid obstacles in multiple

directions. A stereovision system can evaluate the depth field of the surrounding scene using a dual-camera setup. Ultrasonic sensors are used to get accurate altitude information for takeoff and landing. A time-of-flight sensor can take a picture of its environment using infrared light, which contains the depth information for each pixel. ToF sensors have a very high scanning rate but require their own light source, which makes it very difficult to use them in daylight conditions. Solid-state LIDAR systems provide the advantages of a laser scanner in a smaller package (75 g). The lack of moving parts also makes them suitable for high-speed scanning. They can work in daylight and adverse weather conditions. Data from all these sensors may be combined using data fusion, which increases the accuracy. All these sensors might be adapted or modified, and used individually or in combination, to detect wires and cables and warn pilots of the corresponding danger.

11.2 CONCLUSIONS

- The EIA provides the most comprehensive publicly available high-voltage power lines database for the U.S.
- A comprehensive obstacle data is only available close to airports and large cities.
- Preliminary feasibility studies show that it is possible to create power line grid maps using Google Earth.
- A database of the types of cables used in the power industry is readily available.
- A wire-cutter system is currently not available for most lightweight helicopters. Only the Robinson R66 has a wire-cutter system, designed by Magellan Aerospace (WSPS).
- The effectiveness of the WSPS is a function of aircraft mass, speed, and orientation during impact.
- A wire-strike protection system suitable for lightweight helicopters needs to be developed with weight and cost considerations in mind.
- To design a wire cutter for lightweight helicopters, the cutting and failure mechanisms of a wires and cables need to be analyzed.
- The literature combining contact mechanics, crack growth in cables, and impact dynamics is almost non-existent in the public domain.
- The study of sensor technologies used on UAVs to detect/identify obstacles show that with further developments, certain sensors could be suitable for helicopters and make obstacle/wire warning systems possible

11.3 RECOMMENDATIONS

- Obstacle-avoidance systems that are suitable for lightweight helicopters have to be implemented to prevent wire strikes; however, further technological developments are required to reduce the weight and cost of such systems, to make them viable for use on lightweight rotorcraft.

- It is highly recommended to combine different aspects of structural mechanics (contact mechanics, fracture mechanics, and impact dynamics) to understand the working nuances of a helicopter wire cutter and to facilitate the design of an effective wire-cutter system for lightweight helicopters.

- Since lightweight helicopters are involved in 35.5% of wire-strike accidents, a protective device like a wire cutter, combined with prevention technologies, could significantly increase their safety record.

12. BIBLIOGRAPHY

American Wire Group. (2018). Your Single Source for Wire and Cable Products.

Anderson, T. L. (2005). *Fracture Mechanics: Fundamentals and Applications.* CRC Press, Taylor & Francis Group.

Atkins, T. (2009). *The Science and Engineering of Cutting.* Butterworth-Heinemann.

Burrows, L. T. (1980, June). *Investigation of helicopter Wire Strike Protection Concepts.* Tech. rep., Applied Technology Laboratory, U.S. Army Research and Technology Laboratories (AVRADCOM).

Burrows, L. T. (1982, November). *Verification Testing of a UH-1 Wire Strike Protection System (WSPS).* Tech. rep., Applied Technology Laboratory, U.S. Army Research and Technology Laboratories (AVRADCOM).

Caspers, M., & Mattheck, C. (1987). Weighted Averaged Stress Intensity Factors of Circular-Fronted Cracks in Cylindrical Bars. *Fatigure & Fracture of Engineering Materials & Structures, 9*(5), 329-341.

Chan, N. (1980, August). Cable-cutting device. *Patent(US4215833A)*.

Choi, W. S., & Park, G. J. (1999). Transformation of Dynamic Loads Based on Modal Analysis. *International Journal for Numerical Methods in Engineering, 46*, 29-43.

Cornelio, C. J., & Crocker, K. N. (1999, January). Helicopter electronic system for detecting electric power lines during landing. *Patent(US5859597A)*.

Dassault Systems. (n.d.). Basic Concepts of Fracture Mechanics - Lecture 1. *Basic Concepts of Fracture Mechanics - Lecture 1*.

Dattakumar, S. S., & Ganeshan, V. (2017). *Converting dynamic impact events to equivalent static loads in vehicle chassis.* Master's thesis, Chalmers University of Technology, Department of Applied Mechanics, Gothenburg, Sweden.

Development Seed, W. B. (2018). Mapping the electric grid, Using ML to augment human tracing of HV infrastructure. Retrieved from https://devseed.com/ml-grid-docs/

Emigh, C. F., & Goldin, M. (1983). Tactical wire-cutter system for helicopters. *Patent(US4407467A)*.

Federal Aviation Administration, A. I. (2018, January). Daily Digital Obstacle File (DOF). *Daily Digital Obstacle File (DOF)*.

General Cable. (2017, May). Electric Utility, U.S. Energy Products for Power Generation, Transmission & Distribution, TransPowr® ACSR/TW Bare Overhead Conductor, pp. 110-114. Retrieved from http://general-cable.dcatalog.com/v/Electric-Utility-(US)/#page=116

Griffith, A. A., & Taylor, G. I. (1921). VI. The phenomena of rupture and flow in solids. *Philosophical Transactions of the Royal Society of London*, 163-198.

Hertz, H. (1882). Uber die Beruhrung Fester Elastischer Korper (On the Contact of Elastic Solids). *Journal für die reine und angewandte Mathematik, 92*, 156-171.

Huber, M. T. (1904). Zur Theorie der Berührung fester elastischer Körper. *Annalen der Physik, 14*, 153.

Irwin, G. R. (1962, December). Crack-Extension Force for a Part-Through Crack in a Plate. *Journal of Applied Mechanics, 29*(4), 651-654.

Jeppesen. (2017, june). Jeppesen FliteDeck Pro 3.0/9.0.

Johnson, K. L. (1985). *Contact Mechanics.* Cambridge University Press.

Mahmoud, K. (2007, October). Fracture strength of a high strength steel bridge cable wire with a surface crack. *Theoretical and Applied Fracture Mechanics, 48*(2), 152-160.

McClintock, F. A., & Argon, A. S. (1966). *Mechanical behavior of materials.* Reading, Mass.; Sydney: Addison-Wesley, c.1966.

McKown, J. M. (1989, May). Active cable-cutting assembly for aircraft. *Patent(US4826103A).*

Moon, S.-I., Kim, C. H., Koo, J. C., Choi, J.-B., Kim, Y. J., & Kim, Y. J. (2006, January). Simplified Static Analysis for Shock Behavior Evaluation of Thin Glass Plates. *Solid State Phenomena, 110*, 263-270.

Müllerschön, H., Erhart, A., Anakiev, K., Schumacher, P., & Kassegger, H. (2013, May). Application of the equivalent static load method for impact problems with GENESIS and LS-DYNA. *10th World Congress on Structural and Multidisciplinary Optimization.*

Nagaraj, V. T., & Chopra, I. (2008, September). *Safety Study of Wire Strike Devices Installed on Civil and Military Helicopters.* Report, U.S. Department of Transportation, Federal Aviation Administration.

Nexans. (2003, November). Bare Overhead Conductors AAC, ACSR, ACSR II. *Bare Overhead Conductors AAC, ACSR, ACSR II*.

OEDER. (2015). *United States Electricity Industry Primer.* Tech. rep., U.S. Department of Energy.

Priority Wire & Cable, I. (2016, October). Utility Wire & Cable, AAAC - All Aluminum Alloy (6201) Conductor, pp. 2. *Utility Wire & Cable, AAAC - All Aluminum Alloy (6201) Conductor, pp. 2*.

Prof. B. S. Thompson, M. S. (2005). ME 471 Engineeering Design II. *ME 471 Engineeering Design II*.

Prof. J. E. Akin, R. U. (n.d.). Impact Load Factors for Static Analysis. *Impact Load Factors for Static Analysis*.

Reyssat, E., Tallinen, T., Merrer, M. L., & Mahadeva, L. (2012, December). Slicing Softly with Shear. *Physical Review Letters, 109*(244301), 1-5.

Sabatini, R., Gardi, A., & Richardson, M. A. (2014). LIDAR Obstacle Warning and Avoidance System for Unmanned Aircraft. *International Journal of Computer and Systems Engineering, 8*(4), 711-722.

Schulz, K. R., Scherbarth, S., & Fabry, U. (2002). Hellas: obstacle warning system for helicopters. In SPIE (Ed.), *Laser Radar Technology and Applications VII, 4723.*

Seattle Avionics Software. (2018, May). FlyQ efb - Pilot's Guide, A Practical Guide to FlyQ EFB Version 3.1.

Sih, G. C., Tang, X. S., Li, Z. X., Li, A. Q., & K.K.Tang. (2008, February). Fatigue crack growth behavior of cables and steel wires for the cable-stayed portion of Runyang bridge: Disproportionate loosening and/or tightening of cables. *Theoretical and Applied Fracture Mechanics, 49*(1), 1-25.

Smith, M., Tho, C.-H., & Marimuthu, A. K. (2017, August). Cable cutter system. *Patent(US20160096621A1).*

The Aluminum Association. (1999). *Code words for overhead aluminum electrical conductors.* Tech. rep.

Timoshenko, S., & Goodier, J. N. (1951). *Theory of elasticity.* New York: McGraw-Hill.

Yoshida, H. (2009). *Fundamentals of Underwater Vehicle Hardware and Their Applications.* INTECH Open Access Publisher.

APPENDIX A – AWG STANDARDS

Table A1: American Wire Gauge (AWG) Standards

AWG Number	Diameter (in)	Diameter (mm)	Area (mm^2)
6/0 = 000000	0.580	14.73	170.30
5/0 = 00000	0.517	13.12	135.10
4/0 = 0000	0.460	11.7	107
3/0 = 000	0.410	10.4	85.0
2/0 = 00	0.365	9.26	67.4
1/0 = 0	0.325	8.25	53.5
1	0.289	7.35	42.4
2	0.258	6.54	33.6
3	0.229	5.83	26.7
4	0.204	5.19	21.1
5	0.182	4.62	16.8
6	0.162	4.11	13.3
7	0.144	3.66	10.5
8	0.128	3.26	8.36
9	0.114	2.91	6.63
10	0.102	2.59	5.26
11	0.0907	2.30	4.17
12	0.0808	2.05	3.31
13	0.0720	1.83	2.62
14	0.0641	1.63	2.08
15	0.0571	1.45	1.65
16	0.0508	1.29	1.31
17	0.0453	1.15	1.04
18	0.0403	1.02	0.823
19	0.0359	0.912	0.653
20	0.0320	0.812	0.518
21	0.0285	0.723	0.410
22	0.0253	0.644	0.326
23	0.0226	0.573	0.258
24	0.0201	0.511	0.205
25	0.0179	0.455	0.162
26	0.0159	0.405	0.129
27	0.0142	0.361	0.102
28	0.0126	0.321	0.0810
29	0.0113	0.286	0.0642
30	0.0100	0.255	0.0509
31	0.00893	0.227	0.0404
32	0.00795	0.202	0.0320
33	0.00708	0.180	0.0254

34	0.00631	0.160	0.0201
35	0.00562	0.143	0.0160
36	0.00500	0.127	0.0127
37	0.00445	0.113	0.0100
38	0.00397	0.101	0.00797
39	0.00353	0.0897	0.00632
40	0.00314	0.0799	0.00501